Applied Energy 258 (2020) 114069

Contents lists available at ScienceDirect

Applied Energy

journal homepage: www.elsevier.com/locate/apenergy

Review of wearable thermoelectric energy harvesting: From body temperature to electronic systems

Amin Nozariasbmarz[a,b], Henry Collins[a], Kelvin Dsouza[a], Mobarak Hossain Polash[a], Mahshid Hosseini[b,c], Melissa Hyland[a], Jie Liu[a], Abhishek Malhotra[a], Francisco Matos Ortiz[a], Farzad Mohaddes[a], Viswanath Padmanabhan Ramesh[a], Yasaman Sargolzaeiaval[a], Nicholas Snouwaert[a], Mehmet C. Özturk[a], Daryoosh Vashaee[a,b,*]

[a] Electrical and Computer Engineering Department, Monteith Research Center, North Carolina State University, Raleigh, NC 27606, USA
[b] Material Science and Engineering Department, Monteith Research Center, North Carolina State University, Raleigh, NC 27606, USA
[c] Physics Department, Monteith Research Center, North Carolina State University, Raleigh, NC 27606, USA

HIGHLIGHTS

- A review on human energy harvesting for wearable technologies is presented.
- The physiological aspects of the human body for heat generation are explained.
- Materials to system requirements for thermoelectric generators are discussed.
- Rigid and flexible thermoelectric generators for wearables are presented.

ARTICLE INFO

Keywords:
Self-powered devices
Body heat harvesting
Wearable technology
Thermoelectric generators
Flexible harvester

ABSTRACT

Global demand for battery-free metrics and health monitoring devices has urged leading research agencies and their subordinate centers to set human energy harvesting and self-powered wearable technologies as one of their primary research objectives. After an overview of wearables market trends, different active and passive methods of body energy harvesting for powering low-consumption electronic devices are introduced, and challenges of device fabrication are discussed. The discussion continues with the primary emphasis on thermoelectric generators for body heat harvesting. The physiological aspects of the human body involved in heat generation are elaborated. System requirements and the influence of different parameters on the performance of thermoelectric generators are studied at the material, device, and system levels. Finally, the advancements in the development of rigid and flexible thermoelectric generators for wearable and textile integration are presented.

1. Introduction

Today, communication technologies have connected people more than ever before. The idea of "Internet of Things" (IoT), where devices with embedded electronics, sensors, actuators, and software are connected and interacted via the internet, has just gained a vast amount of attention [1]. Wearable technology has gained great attractions with increasing interest in personal health monitoring [2] and various electronic sensors [3]. A combination of IoT and wearables can improve the quality of life by reducing the cost of healthcare, improving elderly people's life, as well as daily body workout monitoring [4].

The required operational power for wearable devices is typically provided by batteries. However, compared to electronics and sensors that are continuously reducing by size according to Moore's law [5], batteries are still bulky and heavy. Also, they have a limited lifetime and require frequent charging; thus, they restrict the functionality of the wearables. For example, in some health monitoring applications where a twenty-four/seven monitoring is needed, chargeable batteries are not reliable due to the probable disruption in the operation during charging. This may cause a severe lack of data acquisition and restrict medical therapeutics.

Body energy harvesting is the primary alternative for batteries to enhance the functionality of wearable devices and has been the subject of many recent investigations [2–3,6–7]. A large amount of human

* Corresponding author at: Electrical and Computer Engineering Department, Monteith Research Center, North Carolina State University, Raleigh, NC 27606, USA.
E-mail address: dvashae@ncsu.edu (D. Vashaee).

https://doi.org/10.1016/j.apenergy.2019.114069
Received 12 April 2019; Received in revised form 18 October 2019; Accepted 27 October 2019
Available online 20 November 2019

energy is released in the form of motion and heat. Therefore, technologies for body heat harvesting using thermoelectric devices [6,8–12], or motion harvesting using piezoelectric and electromagnetic devices [7,13,14–16] have been central for many investigations. The required power for wearable electronic devices for medical purposes such as wireless real-time monitoring and blood pressure sensors ranges from few microwatts (μW) to more than one watt (W) [17]. The amount of generated power from wearable harvesters depends on the size, position, type, and efficiency of the harvesters.

In addition to the ability to provide the necessary power, body energy harvesters must be comfortable to wear and not limiting the natural function of the body organs. They should not be bulky and heavy or increase the involuntary movement or metabolism of the body. The flexibility of these energy harvesters can be another issue that can limit the functionality of the harvester if it covers a large area of the body [17–18].

The mechanical efficiency of the body is only about 15–30% [19], and most of the energy provided by food is released as heat. Body heat can be a continuous source of energy because the core body temperature is regulated at 37 °C. The total heat dissipated from the whole human body is approximately 60–180 W depending on body activity [18]. If one could capture this energy using thermoelectric devices with a conversion efficiency of ~1%, the generated power would have been ~0.6–1.8 W, which is enough to power many wearable sensors [18]. However, this requires covering the whole body with thermoelectric generators (TEG), which is impractical. Achieving the efficiency of 1% is also challenging due to the practical limitations imposed by wearability conditions. It is more practical to cover only a small part of the body with a TEG, maximize efficiency, and minimize the load power for wearable systems. Therefore, a precise design for the TEG at the materials, device and system level is needed to maximize the harvested energy. Any nonoptimality at these levels can impact the output power. Furthermore, the TEG-body attachment, convenience, weight, and reliability are critical factors that should be addressed when designing the system [10,18].

The future of wearable electronic devices is dependent on reducing their power consumption, increasing their functionality and accuracy, as well as utilizing body energy harvesters to reduce or eliminate their dependence on batteries. The human energy harvesters may not remove the necessity of battery usage in wearables; however, they can decrease the size of batteries or prolong their lifetime or the discharging time. In this review paper, we overview the current market and the trends for wearable technology and different wearable body energy harvesting methods. The focus will be on thermoelectric generators, and the materials, device and system optimizations will be overviewed and the future directions directions of wearable generators will be discussed at the end.

2. Market research for wearable technology

The global wearables market has been forecasted to reach $34 billion in 2020 [20–21]. It is anticipated that only in 2021, 240.1 million units of wearable gadgets will have been delivered worldwide resulting in an 18.2% compound annual growth rate (CAGR) [22]. In North America alone, the appearance of the largest population of senior citizens in the current decade along with the thriving sports market with the projected growth of 13.27% between 2017 ($69.3 billion) and 2021 ($78.5 billion) have inspired global investments in physiological tracking wearables [23–25]. Fig. 1 shows the expected share of wearable devices in the global market between 2018 and 2021 [22]. The global market of thermoelectric generators (TEGs), for development of self-powered metrics, is predicted to reach $547.7 M by the end of 2020 [26]. Advancements in smart textiles, with an anticipated market of $9.3B by 2024, are a driver for the wearable TEG market [27].

3. State-of-the-art wearable devices

Since 2012, the National Science Foundation (NSF) sponsored Center for Advanced Self-powered Systems of Integrated Sensors and Technologies (ASSIST) has been focused on the design, fabrication, and evaluation of self-powered health monitoring wearables with enhanced user comfort, robustness, and inter-device communication via the IoTs. Thanks to the uninterrupted data acquisition, such technologies can improve patient-doctor communication significantly and help preempt or fix health issues more reliably. Fig. 2 shows some examples of the ASSIST heat harvesting prototypes designed to power wearable sensors such as an electrocardiogram (ECG) [28].

Seiko Thermic watch (Fig. 3a and b) was the first commercial body-heated powered wristwatch, which was made in 1998 [29]. The thermal to the electrical conversion efficiency of this watch was about 0.1%; its open-circuit voltage was 300 mV, and the output power was approximately 25 μW over 1.5 °C temperature differential across the thermoelectric modules when the watch was worn. Later in 1999, the Citizen Watch Co., Ltd., also developed a body heat-powered watch using rigid TEGs [30]. For 1°C temperature difference, its open-circuit voltage was 640 mV, and it produced 13.8 μW power (Fig. 3c) [31]. PowerWatch® by Matrix Industries®, shown in Fig. 3d, is a more recent smartwatch that is entirely powered by body heat [32]. The fundamental advances in the development of this watch were associated with the TEGs, power management, and heat transfer design [33].

While wearable TEGs can be used to turn on low-power wearables, they cannot yet provide enough power for high power electronics such as cell phones. Yap et al. [34] studied harvesting heat using TEGs for phone charging applications. They used several TEGs on areas of the human body including the chest, palm, and arm to reach the minimum voltage threshold of 250 mV before being able to use a double step-up converter to achieve 5 V. However, the output power at 5 V was still too low for practical phone charging applications. The power can be increased by collecting heat from larger areas of the body. Powerpocket is a registered trademark by Vodafone for a wearable sleeping bag that enables charging of a cell phone while sleeping [35].

Electroencephalography (EEG) refers to the measurement of electrical activity produced by the brain as recorded from electrodes placed on the scalp [36]. The use of EEG electrodes with integrated body heat harvesting TEGs in textiles has been previously reported [37].

gSkin is a product by greenTEG® that exploits a non-invasive TEG-based heat flux sensor for core body temperature measurements. This sensor measured the amplitude and phase shift of the body temperature to monitor the physiological symptoms and early diagnosis of health issues. While some physiological disorders such as jetlag, narcolepsy, and insomnia affect a phase shift in the cycles of the body temperature, others such as sleep quality and burn-out change the amplitude of the body temperature, as shown in Table 1 [38].

4. Energy harvesting from human body

The human body can be a useful source of energy produced from daily activities like walking, running, and swimming or from metabolic heat dissipation. These energies can be harvested through transducers to produce electric power for small devices. Energy harvesting can be done via active mechanisms such as piezoelectric, electromagnetic, and electrostatic or passive mechanisms including thermoelectric and pyroelectric [39].

4.1. Active energy harvesting

Active energy harvesters such as piezoelectric or electrostrictive devices convert oscillatory mechanical energy to electrical energy when they change shape under the application of external stimuli [40–42]. Such harvesters require some voluntary movement, e.g., pressing a spring or a kind of transducer, demanding a deliberate execution of a

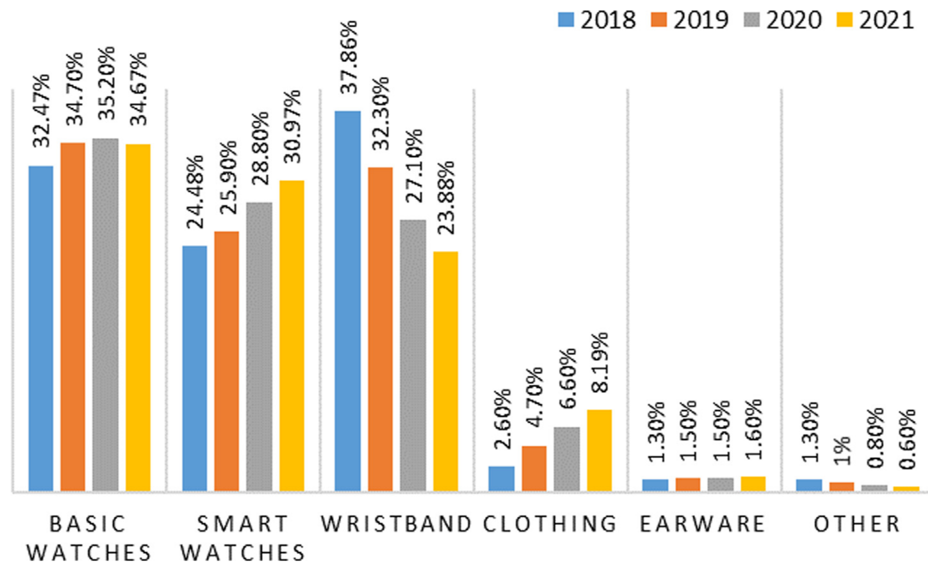

Fig. 1. The share of different wearable devices in the global market between 2018 and 2021. Figure created by authors from the data in Ref. [22].

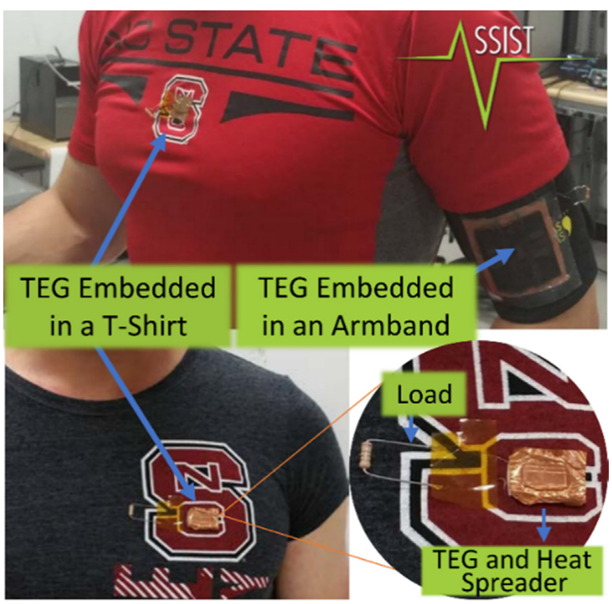

Fig. 2. Thermal harvesting units embedded in a T-shirt and an armband developed in the ASSIST Center. Ref. [28] with permission.

Table 1
Early diagnosis of health issues using gSKIN® TEG heat flux sensors via amplitude and phase shifts of the temperature [38].

Symptom	Amplitude shift	Phase shift
Jetlag		✓
Narcolepsy		✓
Insomnia		✓
Sleep quality	✓	
Burnout	✓	
Alzheimer		✓
Parkinson	✓	
Ovulation	✓	
Sport		✓

specific action that the user would not have done for any other reason than powering the device.

Among the existing ambient energy sources, vibrational energy is considered as one of the reliable sources. It can be transduced into electrical energy utilizing a piezoelectric material, which works based on aligning internal electrical dipoles and creating an electrical polarization [43]. Piezoelectric energy harvesters have high energy densities, reciprocal conversion capability, and simple architectures, which can be formed into microelectromechanical systems (MEMS) [43–44]. To name a few examples, Xue et al. [45] demonstrated a harvester with sputtered bimorph lead zirconate titanate (PZT) capable of generating a power output of 230 μW. In other work, Yeo et al. reported a power

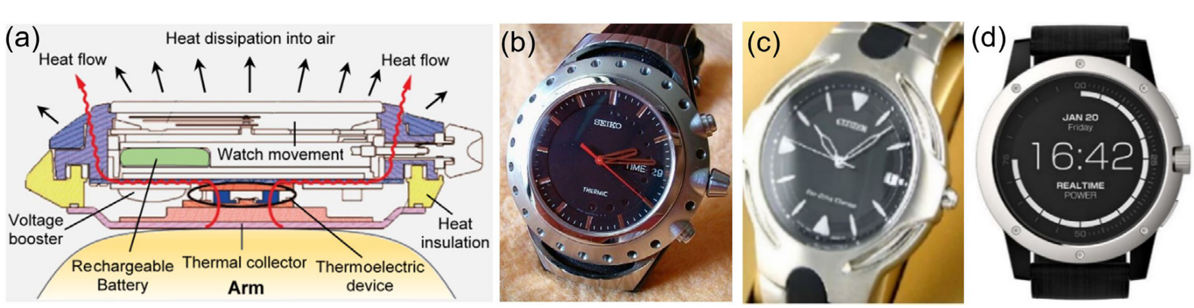

Fig. 3. (a) The schematic of a thermoelectric powered wristwatch concept. The back plate (hot side) acts as a thermal collector receiving heat from the wrist and directing it into the TEG. The watch case (cold front) radiates the heat acting as a heat sink on top of the TEG. (b) Seiko Thermic watch generated about 25 μW from body heat to power the watch [29]. (c) Citizen eco-drive watch generated 13.8 μW power [6]. (d) Commercialized body heat-powered smartwatch made by Matrix Industries [32]. All References with permission.

density of 23.4 μW/cm^2 in a rectangular cantilever unimorph and 64.9 μW/cm^2 in a wrist-worn Bimorph PZT piezoelectric energy harvester [46].

Magnetic induction generators represent another class of ambient energy harvesters and operate according to Faraday's law of electromagnetic induction by converting magnetic energy to electricity via the relative motion of a coil and a magnet [47]. Current studies on improving the power density of microgenerators and their output voltage aim at extending the surrounding area of coils and increasing their magnetic flux density [48]. In the context of battery-less implantable devices, Hannan et al. [49] investigated the means to improve the instrumental reliability, efficiency, and data acquisition rate while reducing the size of the device. Li et al. [50] developed electromagnetic MEMS generating 10 μW at 2 V with an input frequency of 64 Hz. Kymissis et al. [51] measured an average power of 0.23 W in 10 Ω load by placing a magnetic generator outside of a shoe. In another study by Hayashida [52], the average power of 58.1 mW with a peak power of 1.61 W was generated in 47 Ω load using a magnetic generator inside of footwear. Von Büren et al. [53] achieved power densities in the range of 8.7–2100 μW/cm^3 by optimizing type, size and the location of an inertial micropower generator for human walking.

Electrostatic-based harvesters utilize a set of variable capacitor plates, which move by human-body motion. As an example, Roundy reported approximately 0.5–100 mW/cm^3 power density for vibrations in the range of 1–10 m/s at 50–350 Hz [16].

Solar cells [54] and triboelectric generators [55] have been recently used for power generation in wearable devices. Solar cells are solid-state devices that can directly convert light to electricity based on photovoltaic effect. Although the conversion efficiency of the solar cells compared to the other energy harvesters usually is higher, their application in wearables is limited because they can work effectively only under enough ambient light. Their efficiency reduces significantly under the regular indoor lights. Nevertheless, they can charge a storage unit, such as a battery, whenever the wearable receives sufficient light. Numerous research studies have recently shown the potential use of the solar cells in wearables and more work is ongoing [54,56–58].

Triboelectric generators work based on the triboelectric effect, i.e. the common effect of generating static electricity at the contact of two different materials where one works as an electron donor and the other as an acceptor. When a mechanical force is applied on a triboelectric generator, an equal amount of charges with opposite signs are generated on the surface of each contact material [59], which can be stored to later power electronic devices. As an example, Wu et al. [60] reported power density of 3.6 μW/cm^2 for a wearable device. Triboelectric nanogenerators have also recently gained a lot of attention due to their high power densities [61]. For example, Zhu et al. [62], reported power density of 50 mW/cm^2 using a flexible micro-grating triboelectric nanogenerator. Further investigations are focused on solving their limitations such as low currents at high voltages [63]. A summary of the mentioned energy harvesters and an example of their reported high power densities are listed in Table 2.

4.2. Passive energy harvesters

Passive harvesters function based on everyday activities and the released energies from the body without any intention of powering a device. Breathing, blood pressure, and body heat are several primary examples of such energy sources [39–40].

Thermal energy as a significant energy source can be converted into electricity by utilizing either TEGs, which work based on Seebeck effect or pyroelectric generators (PEGs) based on the re-orientation of dipoles triggered by temperature fluctuations [65–66].

Pyroelectric coefficient and Curie temperature under a fixed electric field are the primary selection criteria for choosing materials for PEGs [67]. PEGs can operate in different thermal cycles like Carnot, resistive, synchronized electric charge extraction, synchronized switch damping on inductor (SSDI), and Olsen [68]. Among the mentioned cycles, Olsen and SSDI are the most efficient cycles for activating PEG-based energy harvesters [68]. Yang et al. [69] reported 0.215 mW cm^{-3} power generation from lead zirconate titanate (PZT) PEG films with a thickness of 175 μm. In another study on a PZT based PEG, Potnuru and Tadesse [64] could generate 20 μW upon 5 °C temperature differential. Kim et al. [70] showed that PVDF-based PEGs can produce 0.154 μW power for a temperature difference of 1.5 °C.

Among the passive harvesters, thermal energy harvesters use body heat and do not rely on body motion. They can function uninterruptedly 24 h a day; therefore, they can provide more reliable electrical energy than active harvesters at comparable output power.

The selection of materials for the development of TEGs is often made based on the dimensionless thermoelectric figure-of-merit, zT, associated with each material [44]. Typically, materials with a higher zT are more suitable for thermal energy harvesting [65,71–72] although wearable applications often impose additional restrictions that can be more critical than the zT. Hyland et al. [28] designed BiTe-based TEGs, which could generate a maximum power density of 20 μW/cm^2. Oh et al. [73] showed that 0.1 μm n-WS_2/p-$NbSe_2$ TEGs can produce 0.05 μW/cm^2 from the wrist movement. In another study, a TEG comprising two-dimensional nanosheets of hybrid TiS_2/hexylamine superlattices resulted in a power output of 32 μW/cm^2 at 20 K temperature difference [74]. In a similar study, Shi et al. [75] demonstrated that TEGs based on $Bi_{0.5}Sb_{1.5}Te_3$ and $Bi_2Se_{0.5}Te_{2.5}$ can generate up to 4.07 μW/cm^2 from wrist during walking. The power generated from human body can be significantly enhanced by improving the heat sink or spreader design. Leonov et al. [76] reported the production of 20 μW/cm^2 power density from the human wrist by using Bi_2Te_3 TEGs using a large heat sink. Settaluri et al. [77] generated 21.6 μW/cm^2 power density by adding a heat sink and a heat spreader to Bi_2Te_3 TEGs. To date, the highest power density of 44.2 μW/cm^2 is achieved by the ASSIST Center, NCSU [78], via harvesting the heat from the human wrist by a flexible heat spreader introduced to a nanocomposite-based TEG. Table 3 shows the comparison of performance between different reported TEG systems.

5. Self-powered systems for wearable applications

The system design and the type of transducer being used depend on the nature of energy being harvested. The forms of energy most commonly collected are light via solar cells, heat via thermoelectric generators, and vibration via piezoelectric generators. The power output of each of these transducers varies greatly depending on environmental conditions, creating the need for voltage manipulation and energy storage.

Due to the power fluctuations from the wearable energy harvesting transducers, these transducers cannot be directly connected to the load that they are powering [88]. An entire subsystem (Fig. 4) comprising a rectification circuit, voltage converter, followed by voltage regulation, and finally energy storage must be constructed to take the fluctuating power from the energy harvester and convert it to a steady voltage supply for the wearable device being powered [88–91].

Table 2
Summary of wearable energy harvesting methods.

Energy harvesting method	Power output	References
Piezoelectric	64.9 μW/cm^2	[46]
Magnetic induction	8.7–2100 μW/cm^3	[53]
Electrostatic	0.5–100 mW/cm^3	[16]
Pyroelectric	15.79 μW/cm^2	[64]
Triboelectric nanogenerators	50 mW/cm^2	[62]

Table 3
Comparison between different TEG systems mentioned in the literature.

Author	V_{oc} (mV/cm^2)	Output power	Condition	Location	Ref.
Jo et al.	0.2	0.004 nW/cm^2	No heat Sink	Body	[79]
Wang et al.	37.5	0.08 nW/cm^2	No heat Sink	Wrist	[80]
Jo et al.	0.4	4 nW/cm^2	No heat Sink	Body	[81]
Kim et al.	–	8.1 nW/cm^2	No heat Sink	Chest	[82]
Im et al.	–	46 nW/cm^2	No heat Sink	Chest	[83]
Strasser et al.	–	> 100 nW/cm^2	No heat Sink	Hotplate	[84]
Wahbah et al.	1.6	2.22 μW/cm^2	Large heat Sink	Wrist	[85]
Siddique et al.	0.35	0.01 nW/cm^2	No heat sink, flexible substrate, Cold environment	Arm	[86]
Oh et al.	4.8	0.05 μW/cm^2	No heat sink	Wrist	[73]
Shi et al.	1.88	4.07 μW/cm^2	No heat sink	Wrist	[75]
Hyland et al.	–	20 μW/cm^2	0.13 mm Cu/0.07 mm Carbon film Heat Spreader	Upper arm	[28]
Leonov et al.	–	20 μW/cm^2	Very large heat sink	Wrist	[76]
Wan et al.	–	32 μW/cm^2	No heat sink	Hotplate	[74]
Settaluri et al.	10.8	21.6 μW/cm^2	1.1 mm grooved heat sink and spreader, 2 mm TE legs, natural convection	Wrist	[77]
Nozariasbmarz et al.	–	34 μW/cm^2	anodized aluminum heat sink 25.4 mm × 25.4 mm × 9.5 mm	Arm	[87]
Vashaee et al.	49.7	44.4 μW/cm^2	0.1 mm × 14 cm^2 flexible heat spreaders, 2 mm TEG legs, natural convection	Wrist	[78]

5.1. Boost converters

A boost converter is a power converter that boosts an unregulated input voltage to a higher output voltage. A DC-DC or AC-DC converter depending on the type of the harvester is used to match the input voltage to a level appropriate for the wearable device [88–89]. Some transducers, such as piezoelectric generators, provide AC power; therefore, an AC-DC converter is used [88,92]. Other transducers, such as TEGs, use a DC-DC converter to bring the variable output voltage of the transducer to the appropriate voltage level [88,93–94]. A regulator proceeds to adjust the DC voltage before it reaches the energy storage device [88–89,95]. There are numerous different designs and topologies which can be used depending on the application and type of energy harvester being used. However, the most critical parameter is usually the efficiency of the boost converter, [88], which is $\eta = P_{in}/P_{Batt}$, where P_{in} is the power generated by the transducer, and P_{Batt} is the power that finally reaches the storage after the converter(s) stage losses. In the case of thermoelectric generators, low-voltage start-up is an essential factor. Further, impedance matching between the harvester and the booster is necessary to maximize the output power. A power management unit is also required to load the energy storage unit, such as a capacitor properly, and to power a wearable device, such as a sensor, when sufficient energy is available to run the device. A Li-ion battery or a supercapacitor is often used to store the energy harvested from the transducer [88]. It should be noted that the future of wearable technologies also demands the development of reliable energy storage units. They may require higher energy and power densities, rapid charge/discharge rate, smaller size, flexibility, and longer life-time [96–98].

Because the voltage output of a TEG varies greatly depending on its environment, load impedance matching becomes difficult and leads to variable levels of energy efficiency depending on the power being generated [99]. This is addressed through maximum power point tracking (MPPT), which is a means of tracking the characteristic load impedance that gives the most efficient power transfer under a given power generation scenario [99]. However, MPPT and adding the circuitry needed to make these adjustments create their own efficiency overhead, which can vary from one design to another [99].

As mentioned, another issue with the design of boost converters for self-powered applications is the need for a startup voltage to begin the voltage conversion [100]. Voltage from an external capacitor or vibrations from a switch press can sometimes be used to provide the initial voltage required to start the boost converter [99]. One application was designed such that it could achieve a self-startup using an LC white noise and a positive feedback loop, thereby eliminating the need for an external power supply to provide the startup voltage [99].

Many designs are now being developed to incorporate multiple types of energy harvesting in a single system to compensate for the liabilities of any one method of energy harvesting [101]. This provides more consistent power to the applications being used but comes at the cost of increased design complications and overhead to account for the multiple circuits that are needed to harvest energy from various sources [101]. One design attempted to overcome this challenge by making use of a single inductor for three energy harvesting circuits to avoid redundancy and increase the efficiency of the design [101]. Table 4 compares the efficiency of several power-management units reported in the literature [99–103].

6. Body temperature and skin thermal resistance

The human body maintains a core temperature ranging between 36.5 °C and 37.5 °C [105]. This is achieved by keeping the balance between the energy generated due to metabolism and the heat dissipated to the environment through convection, radiation, and evaporation [106]. The core temperature, controlled by circadian rhythm, varies periodically during the day within the range mentioned above, with a high of 37.5 °C from 10:00 am to 6:00 pm and low of 36.5 °C from 2:00 am to 6:00 am [107]. The body core temperature is generally independent of ambient temperature due to physiological thermo-regulatory systems [108] discussed below:

The thermal conductivity of the skin is reported to be in the range of 0.26–0.3 W/mK depending on the skin temperature and thickness [109]. Heat exchange with the environment takes place through the

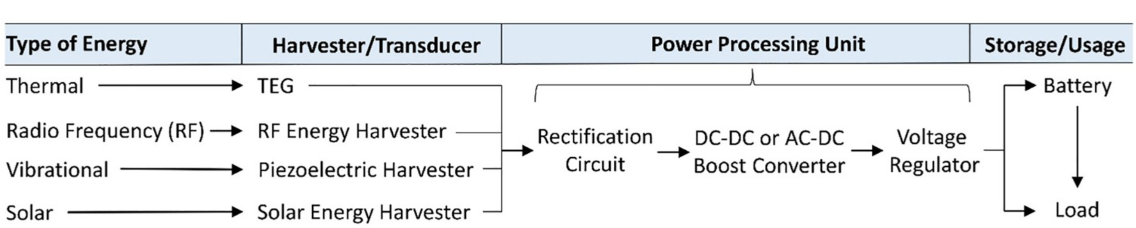

Fig. 4. Diagram of energy harvesting system components.

Table 4
Performance and feature comparison between TEG energy harvesting circuits.

Harvested Energy	Startup Voltage	Startup Method	MPPT Used*	V_{out}	Max P_{out}	Max Efficiency	Ref.
Thermal	40 mV	Positive Feedback & White Noise	Yes	2 V	600 µW (V_{in} = 500 mV)	61%	[99]
Thermal	20 mV	External Voltage	No	1 V	175 µW (V_{in} = 100 mV)	65%	[100]
Thermal, Solar, Vibration	20 mV	External Voltage	Yes	Not Stated	1.3 mW (V_{in} = 160 mV)	64%	[101]
Thermal, Solar	220 mV	RF Kick-Start	Yes	1.1 V	22 mW (V_{in} = 300 mV)	83%	[102]
Thermal	70 mV	Startup Capacitor	No	1.25 V	62.5 µW	58%	[103]
Thermal	60 mV	Self-starting low voltage oscillator	No	4.7 V	220 µW	69%	[104]

* MPPT: maximum power point tracking.

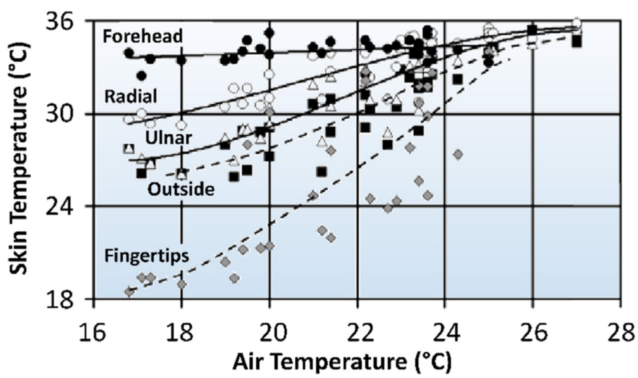

Fig. 5. Variation of skin temperature at the wrist, forehead, and fingertips with respect to an environmental temperature of 20 °C. Ref. [112] with permission.

skin interface [105]. The amount of this heat is controlled by vasodilation and vasoconstriction [110]. Since blood transports heat, small changes in skin blood flow can affect the amount of heat being exchanged with the environment significantly [111]. Fig. 5 shows the variations in skin temperature at different locations on the human body with respect to air temperature [112].

Different parts of the human body can be geometrically modeled as concentric cylinders with each layer representing bone, muscle, fat, dermis, and epidermis (Fig. 6) [113–115]. One of the first heat transfer models assuming isotropic blood perfusion was developed by Pennes [116]. Other proposed models involve more parameters such as arterial temperature variation during branching, blood perfusion anisotropy, counter-current heat exchange, and directional convection [117,118].

Heat loss mechanisms can be either active or passive [105]. In the case of the human body, a passive system consists of convective and radiative losses, which are uncontrollable by the body and depend on ambient conditions [105]. The convective heat loss can be calculated using Newton's law of cooling and depends on the skin roughness and dynamic hair shaft mechanism [119]. Radiative losses can be determined using Stephen-Boltzmann Law. On the other hand, an active system maintains the core temperature by controlling the blood flow rate through skin, sweating, and shivering [105]. Different mathematical models based on active mechanisms have been proposed in the literature [119–121].

7. Thermoelectric generators (TEGs)

The thermoelectric phenomenon has been known since the discoveries made by Seebeck in 1821, followed by Peltier in 1834 and Thomson in 1851. Thermoelectric materials provide reliable conversion of heat to electricity and vice versa [122–123]. The quality of the thermoelectric materials is introduced by the dimensionless figure of merit, zT, according to

$$zT = \frac{S^2\sigma}{\kappa}T \tag{1}$$

where S is the Seebeck coefficient, σ is the electrical conductivity, κ is the thermal conductivity (including lattice component κ_l, electronic component κ_e, and bipolar component κ_{bi}), and T is the absolute temperature [124–125]. According to Pisarenko relation [126], higher carrier concentration, leading to higher σ, results in lower S, while crystal defects reduce both κ and σ. Therefore, zT components are interrelated and require careful optimization of the material properties to improve.

A thermoelectric module is an array of p- and n-type semiconductors, which are electrically in series and thermally in parallel [127]. A thermoelectric module can be used either as a cooler, based on the Peltier effect, or a power generator, based on the Seebeck coefficient. Generally, the efficiency of the generator can be enhanced via increasing zT [127], which is the focus of many investigations in the realm of thermoelectric technology [127–131]. The conversion efficiency (η) of a TEG is a fraction of Carnot efficiency, the maximum efficiency for a reversible cycle, which is calculated using [127]:

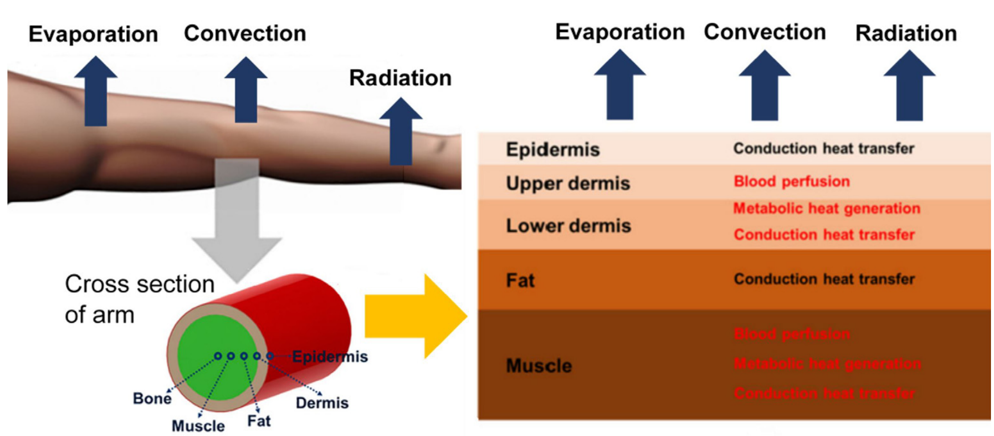

Fig. 6. Illustration of different aspects of modeling of the human body. Ref. [114,115] with permission.

$$\eta = \frac{T_H - T_C}{T_H} \frac{\sqrt{(1 + ZT)} - 1}{\sqrt{(1 + ZT)} + T_C/T_H} \quad (2)$$

where T_H and T_C are the temperatures of the hot and the cold sides, respectively. The term $(T_H - T_C)/T_H$ is the Carnot efficiency, and ZT is the dimensionless figure of merit for the thermoelectric module. Note that zT (with lower case z) is used to represent the material's figure of merit and ZT (with upper case Z) for the device's figure of merit [132]. Due to parasitic effects, mainly from metal contacts, ZT is generally less than zT [133]. Therefore, it is ultimately the device ZT that must be maximized for the working temperature to deliver maximum power and efficiency.

7.1. TEG materials requirements for wearables

To ensure the high performance of a wearable heat harvesting platform, the embedded TEG must be optimized on materials, devices, and system levels. In addition to high zT, the material must have low thermal conductivity to increase temperature gradient ($\Delta T = T_{hot} - T_{cold}$) across TEG [2]. This requirement is mainly due to the skin thermal resistance and the constraints for using a large heat spreader in a wearable platform [8]. For the integration of the TEGs in a wearable electronic device, the material must also have a high Seebeck coefficient to generate a useful voltage for the efficient operation of the subsequent DC-DC boost converter [134].

Among the known thermoelectric materials, bismuth telluride-based alloys are the best candidates for room-temperature applications. They have been extensively developed in the last few decades. Fig. 7 compares room temperature Seebeck coefficient, thermal conductivity, and zT of the state-of-the-art p-type $(Bi_xSb_{1-x})_2Te_3$ [135–140] and n-type $Bi_2Te_{3-x}Se_x$ alloys [141–149].

Although some of these alloys show zT > 1, they do not fulfill the material requirement for wearable applications. In comparison to the commercial alloys [135,141], nanostructured materials mainly provide smaller thermal conductivity and higher zT [134–135,138–139,144–146,149–150]. Therefore, nanostructured $(Bi_xSb_{1-x})_2Te_3$ and $Bi_2Te_{3-x}Se_x$ alloys are the best candidates for body heat harvesting applications.

Rigid TEGs have been traditionally used for power generation. Properties of the constituent materials determine the efficiency of rigid TEGs. For example, in comparison to p-type, n-type alloys show weaker thermoelectric properties at room temperature (Fig. 7). N-type alloys theoretically suffer from low zT due to the smaller number of valleys near the conduction band edge. Further improvement in the efficiency of the rigid TEGs for a wearable application requires enhancement in zT together with a reduction in the thermal conductivity of n-type $Bi_2Te_{3-x}Se_x$ alloys and p-type $(Bi_xSb_{1-x})_2Te_3$. Historically, the main challenge in materials requirements is zT improvement. This requires more experimental research and breakthroughs to obtain zT > 2 at room temperature for both n- and p-type materials to improve the efficiency near the body temperature. Recently, researchers are focusing on flexible and printable TEGs [151–153]. These devices are generally less efficient than rigid TEGs; however, their flexibility makes them attractive for wearable and textile integration applications.

7.2. TEG device requirements for wearables

At the device level, careful consideration must be paid to several factors in the design of TEG devices to maximize their power output. These factors include thermal load matching [12,154–155], the effect of heat spreaders [8,28] choices of filler material(s) [156–160], type of metal interconnects, and substrate [151,161–165], and thermoelectric leg geometry [8,166–167].

7.2.1. Filler material

Lateral heat losses through fillers can reduce the ΔT and impair the TEG power output [112]. The ratio of the planar area taken up by the thermoelectric material over the total surface area of the module is called the fill factor [168]. For example, for a device with a fill factor of 10%, thermoelectric leg thermal conductivity of 0.3 W/mK, and filler conductivity of 0.03 W/mK, the total thermal conductance of the thermoelectric material and that of the filler are equal; hence, half of all heat is lost through conduction in the filler lowering the power output. Finding fillers with minimal thermal conductivity is crucial to improving the power output of a TEG. Air is a convenient TEG filler material with a low thermal conductivity of about 0.024 W/mK and does not require an airtight seal [158]. Silica aerogels are excellent thermal insulants with a potentially lower thermal conductivity than that of air

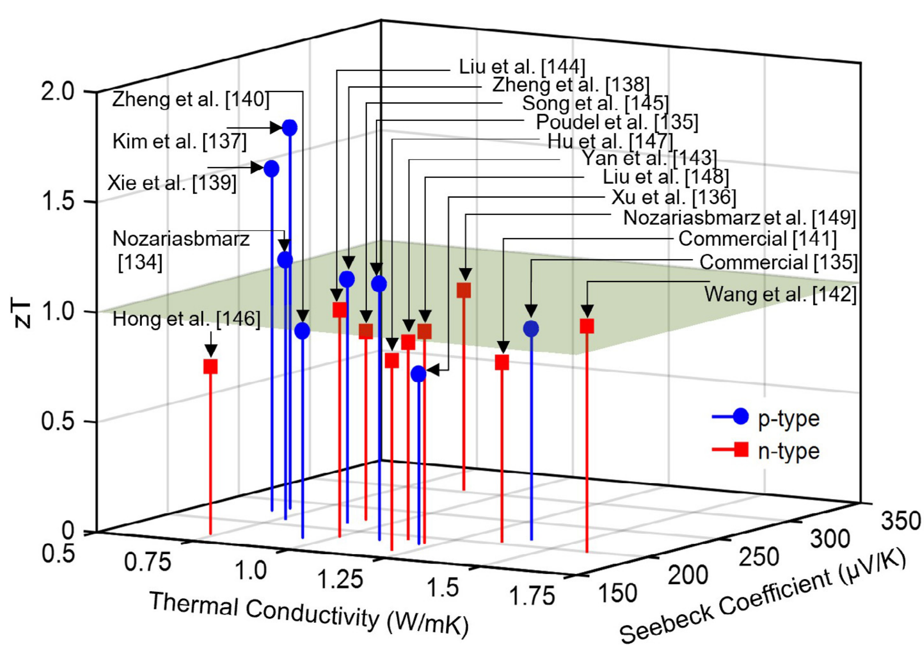

Fig. 7. Comparison of the room temperature Seebeck coefficient, thermal conductivity and zT of the state-of-the-art p-type $(Bi_xSb_{1-x})_2Te_3$ [134–140] and n-type $Bi_2Te_{3-x}Se_x$ alloys [141–149].

Table 5
Specific skin resistance, skin/object resistance, and contact area reported in the literature.

Specific skin resistance	Skin/object resistance	Contact area	Ref.
6.25×10^{-3} Km^2/W	125 K/W	50 mm^2	[169]
5.6×10^{-3} Km^2/W	110 K/W	50 mm^2	[109]
1.1×10^{-2} Km^2/W	12.2 K/W	900 mm^2	[10]
3×10^{-2} Km^2/W	–	–	[155]
1×10^{-2}–5×10^{-2} Km^2/W	–	–	[170]
5.4×10^{-2} Km^2/W	–	–	[171]

capable of improving structural integrity while adding minimal mass to the module [156,159–160].

7.2.2. Thermal load matching

The device performance is dictated by TEG thermal resistance, which must be high and comparable to the parasitic thermal resistances in series with the TEG. The TEG thermal resistance can be enhanced by reducing the fill factor, i.e., reducing the number of p- and n- legs, increasing the aspect ratio of the legs, and/or decreasing the thermal conductivity of the legs [8].

Three primary sources of thermal resistances at the skin-TEG and TEG-ambient interface can limit the TEG device performance: (1) human skin, known as a thermal insulator, results in resistance between the TEG and body core. (2) The contact resistance between the interface of the skin and TEG due to the surface roughness of the skin. (3) The thermal resistance at the interface of TEG and ambient, which depends on air convection [8]. This TEG-air interface resistance is often the dominant thermal resistance if no heat sink is used on top of the TEG. The thermal resistance, which is a determinative parameter for body heat exchanges, is estimated with experimental equations, and it can be varied by skin characteristics and contact pressure [109]. The maximum generated power from a TEG can be decreased by ~30% when it is located on body skin [10]. Table 5 shows a list of specific skin resistance, skin/object resistance, and contact area reported in the literature.

From the thermal circuit perspective, the thermal generator consists of a human body and air, and a thermal load includes a TEG and its corresponding parasitic resistances (Fig. 8) [154]. Thermal resistance matching between the TEG and the thermal generator is vital for maximizing power output [155]. The optimal thermal resistance of a TEG is defined as [112,172]:

$$R_{TEG,Optimal} = \frac{R_F(R_{skin} + R_{air})}{2(R_{skin} + R_{air}) + R_F}$$

where R_F is the parasitic thermal resistance due to the filler material in parallel with the TEG, R_{skin} is the thermal resistance between the body core and the surface of the skin, and R_{air} is the thermal resistance of the ambient air.

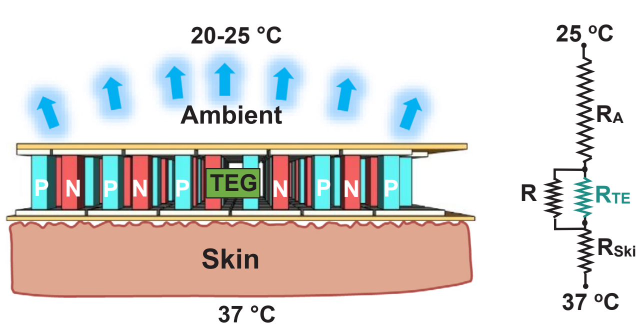

Fig. 8. TEG Thermal circuit for body heat harvesting. R_{skin}, R_{TEG}, R_F, and R_{Air} are the thermal resistance of the skin, TEG, the filler thermal resistance, and the air, respectively.

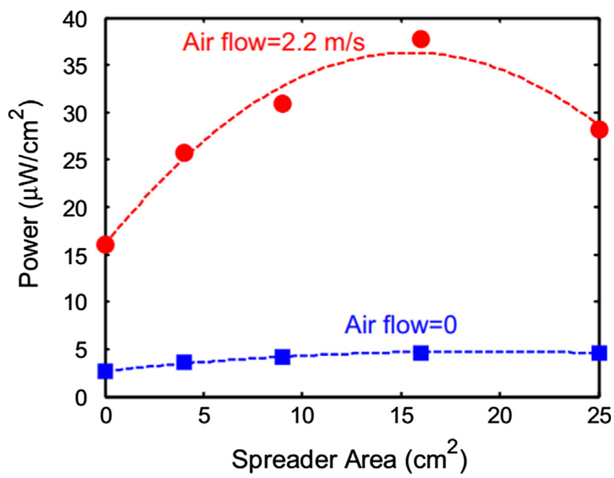

Fig. 9. The effect of the heat spreader surface area on the power output of TEGs under two conditions of with and without airflow. Ref. [28] with permission.

7.2.3. Heat spreaders

The overall performance of a wearable TEG can be improved by using heat spreaders. The advantage of a heat spreader compared to a fin heat sink is its lower weight and flexibility, which is desired for wearable applications. Heat spreaders with high thermal conductivity can be placed on both the cold and hot sides of a TEG to enhance the power output. For example, carbon and copper foils, with thermal conductivity (κ) of ~1000 W/mK and ~400 W/mK, and thickness (t) of ~100 μm and ~250 μm, respectively, have been used as heat spreaders to maximize the generated power [28]. The results did not show a significant difference between these two materials, which can be understood considering similar κt factor. As shown in Fig. 9, increasing the surface area of a spreader raises the power output up to a certain point, after which the lateral thermal resistance begins to dominate, and the role of the spreader becomes less significant. According to the experimental results [28] and the analytical modeling [8], the optimum heat spreader size for this case was 4 cm × 4 cm. Compared to a TEG without the heat spreader, the output power increased by 100% using a 16 cm^2 spreader.

7.2.4. Metal interconnects and substrates

As mentioned, a TEG consists of p- and n-type thermoelectric legs which are electrically in series. The electrical connection between the legs is through metal interconnects mounted on an insulating substrate, usually a ceramic. Metal interconnects should possess high electrical conductivity and a matching thermal expansion coefficient as that of the thermoelectric legs [161]. Typically, they are made of copper or gold-coated copper that can be as thin as 20 μm. The interfacial contact resistance between the legs and the interconnects can limit the device performance if the leg resistance becomes comparable to the contact resistance. This usually happens if the contact resistance exceeds 10% of ρL/2, where ρ is the electrical resistivity, and L is the length of the leg. For example, for a Bi_2Te_3 leg with $\rho \sim 10^{-3}$ Ω cm, and a contact resistance of 10^{-6} Ω cm^2, the leg length should be above 0.2 mm [173].

In rigid TEGs, legs and interconnects are typically affixed to a highly thermally conductive ceramic substrate, such as alumina (κ ≃ 30 W/mK) or aluminum nitride (κ ≃ 285 W/mK) [164]. In flexible TEGs, the eutectic alloy of gallium and indium (EGaIn) as a liquid-metal interconnect has offered both flexibility and self-healing properties, ensuring the integrity of the module even after experiencing severe strains [151]. The two substrates mostly used in flexible devices are polydimethylsiloxane (PDMS) and Kapton HN. Flexible substrates, compared to the rigid ones, can impede heat flow from the human body to the TEG due to their higher thermal resistance [151,165].

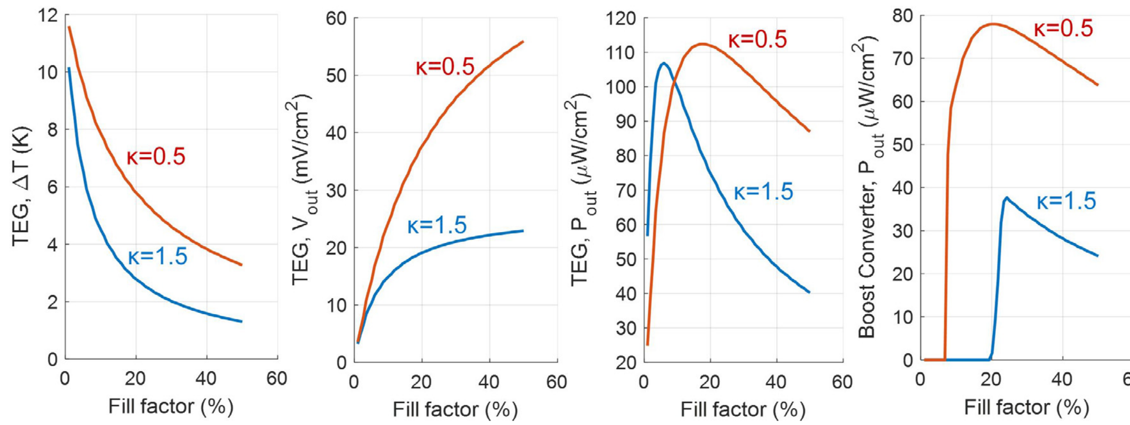

Fig. 10. Effect of varying fill factor on ΔT, TEG output voltage, TEG output power, and boost converter output power for given thermal conductivities of κ = 0.5 W/mK, and 1.5 W/mK.

7.2.5. Number of legs and leg geometry

A large number of legs results in a reduction of TEG thermal resistance and ΔT. For example, on a human body condition, for a low thermally resistive TEG module, once the fill-factor is higher than about 10%, the maximum ΔT is less than 2 °C in a typical commercial bismuth telluride thermoelectric devices [8]. By increasing leg length (aspect ratio), altering leg shape, and decreasing fill factor, ΔT across the module, and thus output power can be improved [8,174]. It should be noted that although a smaller fill factor is desirable for higher power, e.g., as a module with a fill factor between 0.3 and 3% can produce over several times more power per unit area than devices with fill factor of above 25% [167], a module with a fill factor of < 20% may compromise the mechanical integrity [8]. For systems with a small ΔT, rectangular legs are optimal for maximum power generation [166]. The effect of the fill factor on ΔT, TEG voltage, and TEG power output is shown in Fig. 10. The quantities are calculated for a TEG with rectangular legs of $0.6 \times 0.6\,mm^2$ cross-section area and 2 mm height using a similar model as in ref [8]. The p- and n-type materials' figure-of-merits are assumed to be 1 and 0.7, respectively, similar to typical commercial bismuth telluride-based materials. Seebeck coefficients are considered to be 200 μV/K for both materials. Two values of thermal conductivities are considered, 1.5 W/mK and 0.5 W/mK. The electrical conductivity is adjusted to keep the same values of zTs for both TEGs. A heat spreader of $10\,cm^2$ on top of the TEG and natural convection is assumed. It can be seen that FF ~ 6% results in the highest value of TEG power output for κ = 1.5 W/mK (e.g., a typical commercial thermoelectric device). This value increases to FF ~ 18% for κ = 0.5 W/mK with almost similar peak TEG power output. However, for the first TEG (κ = 1.5 W/mK), the DC-DC boost converter has zero power output at FF ~ 6% due to the small TEG voltage output, which is not sufficient to turn on the boost converter. The boost converter power output shows a strong dependency on the material's thermal conductivity for the same reason. It is, therefore, essential that the TE material and the TEG device parameters should be optimized to maximize the power available to the system at the output of the boost converter (not the output of the TEG).

Fabrication of TEG devices is a challenging process. Along with the optimum design of the device, which discussed earlier, the headers material, quality of the interconnects, contact resistance between TE legs and interconnects, repeatability, and mechanical properties of TEGs are highly effective on device performance and efficiency. Further improvement in body heat harvesting directly depends on minimizing the contact resistance of TE legs and maximizing the stability of the modules at different environments and infinite energy generation cycling.

7.2.6. Environmental effects

Environment temperature and air velocity are the two main factors that influence the generated power from the TEG. As discussed in Section 6, the core body temperature is usually independent of the ambient temperature due to the physiological thermo-regulatory system. Therefore, the skin surface temperature is a small function of the ambient temperature and does not change significantly with the environment. When the ambient temperature increases and is below the surface body temperature, the ΔT across the TEG decreases. In a warm climate that the ambient temperature rises above the surface body temperature (~33–35 C), the TEG can still produce power. In such cases, a bipolar boost convertor can regulate the polarity of the output voltage. Only when the ambient temperature is precisely equal to the skin temperature, the TEG cannot produce power because there is no ΔT across the TEG. In addition to external parameters, thermoelectric material properties are also functions of temperature. However, their variation is usually small over the typical changes in the ambient temperature.

Air velocity is another critical factor that affects the TEG performance. Higher air velocity can enhance the generated power significantly due to a higher heat rejection from the cold side. The heat rejection saturates at very high air velocity. Suarez et al. [8] showed that at the air velocity of 0.9 m/s, 5× more power than steady-state condition can be achieved (Fig. 11).

It is worth knowing that other environmental effects such as humidity and air pressure can also affect the TEG performance; however, their influences have not been yet studied in the literature.

8. Flexible TEGs

Flexible TEGs have been of interest for wearable applications due to their lightweight, low thermal resistance, breathability, long-term

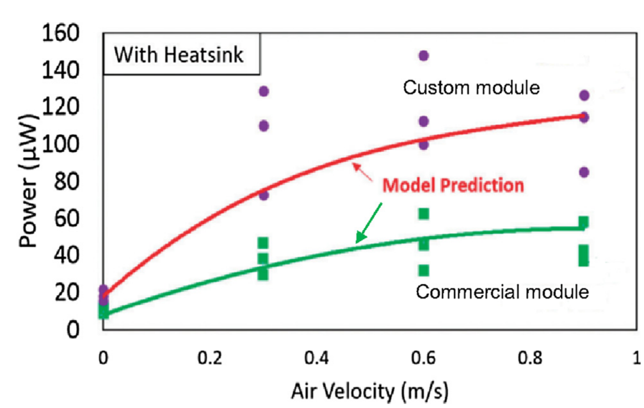

Fig. 11. Experimental comparison of generated power versus air velocity for commercial and custom thermoelectric modules. Ref. [8] with permission.

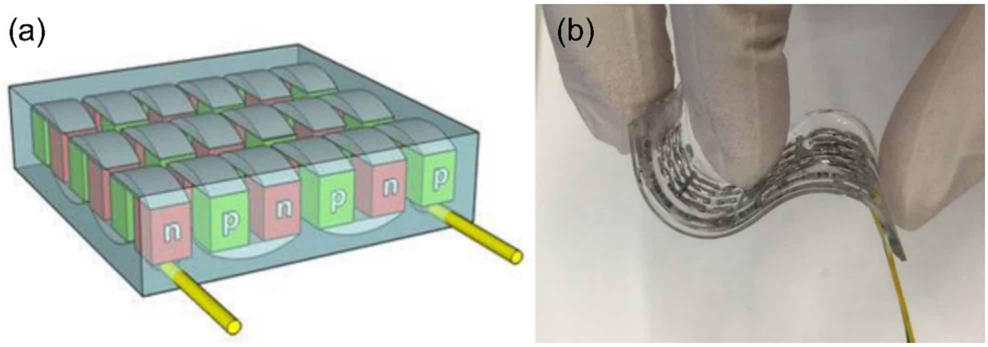

Fig. 12. (a) Schematic and (b) a fabricated flexible TEG using bulk thermoelectric legs embedded in PDMS and connected with liquid metal. Ref. [151] with permission.

Table 6
Summary of generated power outputs reported in the literature.

Technique	Year	ΔT/Ambient	Power ($\mu W/cm^2$)	Ref.
Bulk Materials	2017	Ambient = 5°C	8.75	[151]
Bulk Materials	2017	Ambient = 20°C	3.2	[152]
Bulk Materials	2017	ΔT = 1°C	2	[184]
Bulk Materials	2018	Ambient = 25°C	7.31	[185]
Bulk Materials	2018	Ambient = 24°C	5.6	[186]
Electrodeposition	2018	Ambient = 15°C	3	[193]
Fabrics	2016	ΔT = 10°C	2	[192]
Fabrics	2015	ΔT = 72°C	0.0006	[191]
Organic Solution	2016	Ambient = 5°C	0.03	[190]
Screen printing	2016	ΔT = 1°C	7.3	[194]

comfort, high coverage on the skin, ease of incorporation to fabrics, and conformal contact to the skin while being aesthetically pleasing [162,175–176]. Such TEGs can be fabricated by methods such as printing [175,177], lift-off [178], flash evaporation [179], and electrochemical deposition [162] with integration into various substrates including nanowires [180], thin films [181], coils [182], CNTs [179], bulk flexible matrices [175], and textiles [28,183].

Bulk thermoelectric legs can be integrated into a flexible platform using elastic interconnects. Eom et al. [152] created a modular bracelet-like wristband device using bulk thermoelectric material blocks. The device consisted of ten small rigid thermoelectric legs, which were connected via flexible copper wires and elastic polymer links, allowing for structural flexibility across the module. Jeong et al. [184] explored the use of Eutectic Gallium-Indium, which is liquid at room temperature, as a flexible and stretchable interconnect between bulk thermoelectric legs. Suarez et al. [151] created flexible TEGs using bulk commercially available Bi_2Te_3-based legs connected electrically with EGaIn. The whole structure was embedded in PDMS for mechanical robustness. Jo et al. [79], used Bi_2Te_3 in PDMS and incorporated flexible electrical circuit boards as interconnects. Kim et al. [185] fabricated a flexible TEG using bulk thermoelectric legs, soldering paste interconnects, and a proprietary filler polymer with a low thermal conductivity of 0.03 W/mK. Fig. 12 shows an example of a flexible TEG made with bulk rigid thermoelectric legs embedded in a flexible substrate.

Park et al. [186] built a fully flexible TEG by placing bulk bismuth telluride legs inside Bakelite holders. In their design, holders were connected via flexible wires, thermoelectric legs were interconnected via a flexible printed circuit board (FPCB), flexible thin films of deposited Ni/Au were attached to thermoelectric legs using soldering, and a solid-state cooling gel was used on the cold side to perform as a heat sink.

Organic and solution-based materials can be used in thin-film thermoelectric devices [187–189] to make them breathable and provide long-term comfort. Yang et al. [190] constructed a device using poly vinyl alcohol (PVA) gel electrolytes doped with ferric chloride and potassium ferricyanide. Oh et al. [73] proposed a device fabricated with exfoliated transition metal dichalcogenide nanosheets on top of a PDMS substrate and used Ag and Au wires as electrical interconnections. Du et al. [191] coated polyester fabric with a PEDOT:PSS solution and fabricated a planar device. The coated polyester strips were attached to a larger polyester substrate by silver paint, and finally, silver wires were used for electrical interconnection between each strip. Lee et al. [192] made a device with nanofibers coated with n- and p-type Bi_2Te_3 sheaths. Polyacrylonitrile (PAN) nanofiber sheets were sputtered a final Au film connecting n- and p-type sheets. The flat sheet was twisted into a single fiber containing alternating sections of the thermoelectric material. Huu et al. [193] grew wide lateral legs on a flexible substrate and connected them vertically to the hot and cold side using copper studs. This TEG had the advantages of a vertical device, and at the same time, material growth could be controlled more reliably. Kim et al. [194] created a vertical device utilizing screen printed top and bottom copper contacts on Ni coated Si wafers. The thermoelectric legs were made using a ball-milled ternary bulk thermoelectric materials. The legs were coated with an additional Ni layer to reduce the electrical contact resistance between the legs, and Sb/Au paste, which bonded the copper interconnects and the legs. Table 6 represents a summary of the power levels for the mentioned flexible TEGs.

The primary challenge of the flexible TEGs is their lower output power. For most of the cases, the high power is sacrificed for flexibility. New ideas are demanded to make the generated power from flexible TEGs comparable to rigid ones while the flexibility is maintained. Attachment of a miniature and reliable heat sink, or a capable heat spreader, can enhance the flexible device performance as for the case of rigid TEGs.

8.1. Flexible TEGs with rigid interconnects

To ensure proper contact at the device and skin interface, and thus higher output power, Liu et al. [195] fabricated wearable TEG devices with optimized heat spreaders via packaging the bulk thermoelectric legs in the flexible thermal spreaders. Fig. 13a shows the device in which thermoelectric legs were soldered directly onto the layer of metal contact deposited on a flexible PDMS substrate [195]. The challenge in the fabrication of this device was the cracking of the layer of the metal contact, and thus losing conductivity when the substrate was subjected to stretching and bending. The PDMS substrate was steam-etched and cured to create a porous surface to address this challenge. Despite partial cracking in the metal layer, this technic helped to preserve alternate channels across the layer allowing for electrical conductance during stretching and bending. The output power of the fabricated TEG under different airflow speeds is shown in Fig. 13b [195]. The generated power output was between 1 and 8 $\mu W/cm^2$ at different airflow speeds ranging between 0 m/s and 7 m/s. The metal interconnect in this device was 500 nm thick, which resulted in high electrical resistance. The power can be improved by using thicker metal interconnects [195].

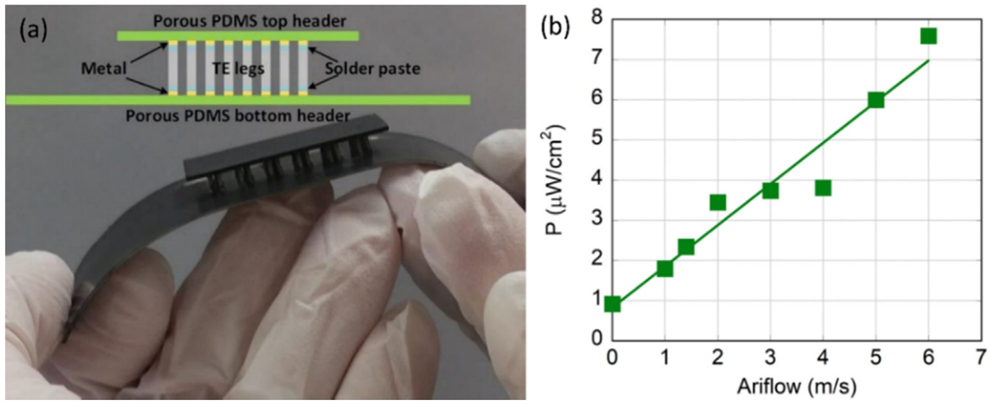

Fig. 13. (a) A flexible TEGs with rigid interconnects, (b) The output power of the TEG at different airflows. Adapted from Ref. [195] with permission.

9. Integration of harvesters in textiles

TEG-incorporated textiles can address some limitations such as the lack of wearability, mechanical stability, foldability, flexibility, washability, and lightweight while transducing a range of energies based on triboelectric, piezoelectric, photovoltaic, and thermoelectric effects [196]. AiQ Smart Clothing®, MYANT®, and Ohmatex® are companies that are developing physiological and environmental sensors for integration into sportswear, medical devices, and protective clothing [197–199]. Their R&D focuses on aspects such as fiber fabrication, design, and body placement to maximize power output, comfort, and durability. The ASSIST center at North Carolina State University is working on the integration of electronic sensors and TEGs in textiles for health and environmental monitoring applications [2,28].

In a review by Zhang et al. [200], state-of-the-art fiber-based TEGs have been compared from different standpoints, including operational principles, fabrication methods, materials, characterization, device structures, and potential applications. Two critical criteria in the design of TEG-incorporated textiles are the location of the TEG unit on the body and the capability of maintaining both adequate airflow and ambient temperature differential to produce maximum output power [28,201]. Fig. 14 shows the variations in the power generated by a bulk TEG at different body locations (upper arm, wrist, chest, and T-shirt) when exposed to different air velocities ranging from 0 to 1.4 m/s [28].

Kim et al. [202] developed a fiber composite TEG comprising carbon nanotubes (CNT: 10–50 wt%)/poly(3,4-ethylenedioxythiophene):poly(styrene sulfonate) via wet-spinning and post-treatment technics. As shown in Fig. 15a, the design consisted of 12 pairs of p- and n-type thermoelectric fibers connected with silver paste. The temperature difference between the two ends of the fiber was adjusted by Peltier devices, and the Seebeck coefficients and electrical conductivities of the fibers were measured using gold probe tips. The maximum Seebeck coefficient and generated power output power over 10 °C temperature difference were found to be 18 μV/K and 0.430 μW, respectively. The corresponding I-V and P-I curves over the same temperature range are shown in Fig. 15b. These values are obviously too low for any or most practical applications. Under the on-body conditions, the temperature difference will be much less than 10 °C, resulting in even lower voltage and power values.

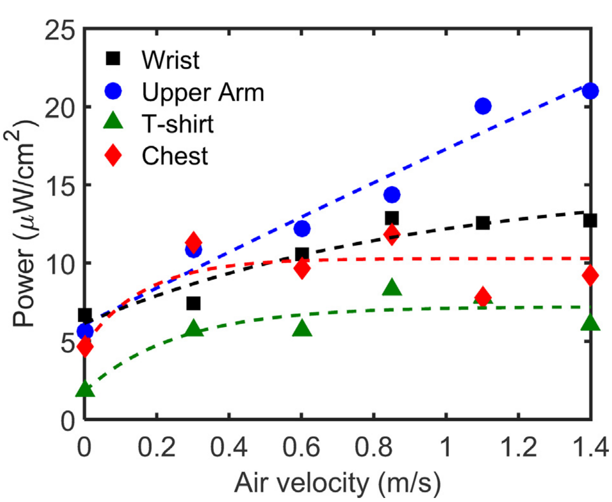

Fig. 14. The power generated by a bulk TEG at various body locations. Ref. [28] with permission.

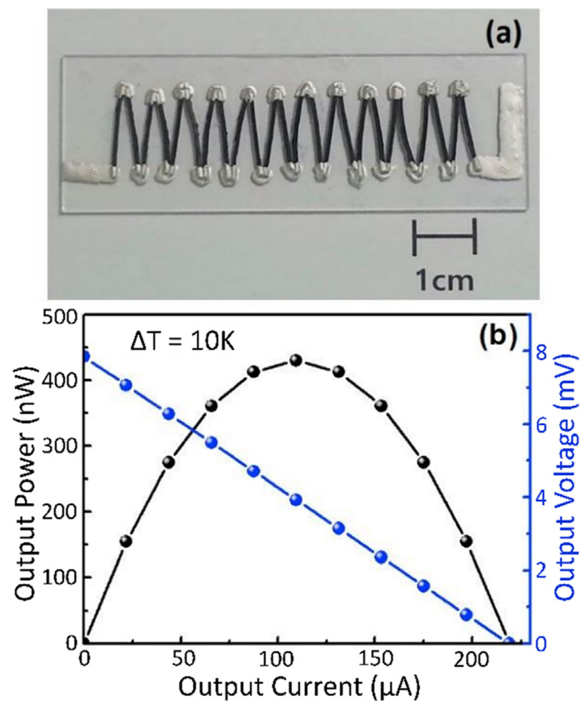

Fig. 15. (a) Photograph of the fiber composite TEG consisted of 12 pairs of n-type, p-type fibers connected with silver paste (b) P-I and IV curves resulting from the 10 K temperature difference between the two ends of the fiber. Ref. [202] with permission.

In another study by Lu et al. [183], p- and n-type thermoelectric materials were hydrothermally synthesized and deposited onto both sides of silk fabric to form thermoelectric columns, which were connected with silver foils to fabricate an array of 12 thermocouples. The silk fabric embedded with thermoelectric legs and the interconnects, shown in Fig. 16a, generated a maximum voltage and output power of approximately 1 mV/cm^2 and 1 nW/cm^2, respectively [183]. Siddique

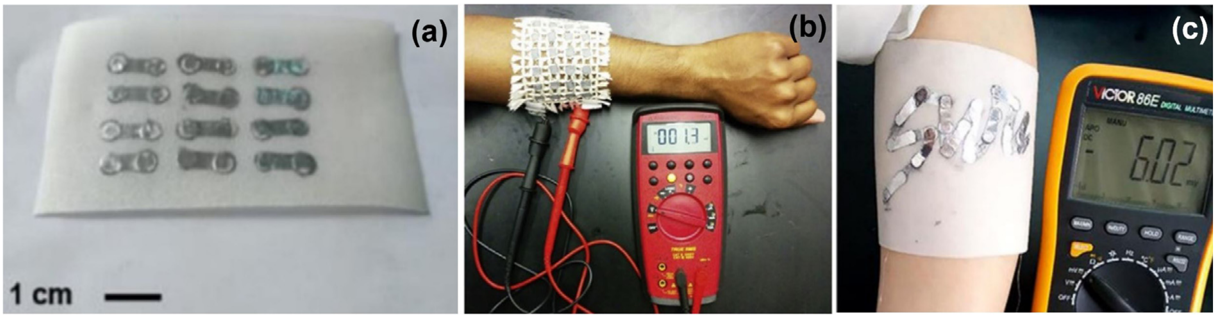

Fig. 16. Several examples of textiles integrated with TEGs. (a) a silk cloth with TE materials deposited on both sides of the fabric and connected with silver foils [183], (b) a polyester clothes embedded with thermoelectric legs manually dispensed out of paste in between the fibers [86], (c) A silk-based TEG [183]. All References with permission.

et al. [86] developed polyester fabric clothes embedded with p-type $(Bi,Sb)_2Te_3$ and n-type $Bi_2(SeTe)_3$ legs of 5 × 5 × 1.4 mm^3 legs. In this process, thermoelectric pastes were first prepared by mixing the thermoelectric powders with Durabond-950 binder. The pastes were manually dispensed in between the polyester fibers and were electrically connected using silver threads. The cloth was subsequently cured at 160 °C for 2 h in a furnace. The fabric was tested at different conditions. A maximum power density of 0.06 nW/cm^2 was measured from the arm. In a similar approach, a polymer-based clothe was fabricated with printed TE materials [203]. In this study, a silver conductive thread was sewn onto the fabric and cut by the location of the TE legs. A thermoelectric paste, made of the mixture of TE powders and the Durabond-950 binder, was dispensed into the spaces among the fibers and subsequently cured at 100 °C for 2 h. The energy generated from the clothing worn by a human subject was approximately 0.054 nW/cm^2.

The screen-printing of thermoelectric films onto fabrics can make a significant leap in scaling-up the TEG-embedded textiles [181,204–205]. Typical printing processes require a large concentration of binder additives, which interfere with electrical transport on printed thermoelectric layers. Shin et al. developed a screen-printing method using a class of methyl cellulose to create printable TE slurries with a low concentration (0.45–0.6 wt%), mitigating the detrimental effect of the binders on electrical conductivity [206]. Wu and Hu [207] developed textile yarns (polyester and cotton) coated with waterborne polyurethane-based thermoelectric composites consisting of 20 wt% MWCNT, 1:4 ratios of MWCNT to PH1000, and 5 wt% DMSO doping. The optimal electrical conductivity, Seebeck coefficient, and the power factor achieved at room temperature were 138 S/cm, 10 μV/K, and 1.41 $\mu W\, m^{-1} K^{-2}$, respectively.

Note that the harvested energy from the textiles-based TEGs is yet so small that even if the whole body is covered with them, they cannot produce sufficient power for wearable applications. The low harvested energy is partially due to the fabrication methods, such as adding binders and printing, that impacts the thermoelectric materials properties. Another important factor is related to thermal management when the TEG is integrated into textiles. Even though there is about 10–15 degrees temperature difference between the core body temperature and the ambient, only a small amount of that drops across the TE legs due to numerous parasitic series and parallel thermal resistance that would reduce the heat available to the TEG. Therefore, the strategies for integration of TEGs in textiles must be implemented according to the tight constraints imposed by thermal management on the human body while maintaining both the body comfort and device reliability.

10. Future directions

The global demand for wearable technologies is anticipated to surpass a $78B market by 2021. The world's growing fascination with performance monitoring has brought the wearables market from bulky powered vests developed in the 1980s to seemingly ubiquitous wristband pedometers and activity monitors. In this sector, efficient body energy harvesters can open new opportunities ranging from battery-less wearable electronics for monitoring of human health and environmental conditions to the sport and recreational gadgets. Watches, belts, headbands, cuffs, smart jewelry, and smart textiles can all provide platforms for monitoring health, wellness, and users' immediate environment. The benefits of networks made with small self-powered devices are truly revolutionary.

Beyond the early applications of activity monitors and pedometers, digital and connected mobile health promises to revolutionize the planning and delivery of medical care and empower health teams to support patient monitoring and recovery. Thermoelectric generators in this regard seem to be closer to commercialization with several wearable products already been introduced to the market, such as Matrix PowerWatch [32], Embr wave thermoelectric wristband [208], and Climaware dhama innovations heat jacket [209].

The integration of energy harvesters in clothing is another direction that is being currently researched and evaluated. In this regard, despite the efforts for inclusion of TEGs in textiles, the power levels are still too low for practical applications. Methods based on bulk TEGs, compared to printed or thin-film approaches, have shown significantly higher power due to their ability to maintain a more significant temperature differential across the thermoelectric junctions. However, they may not have the desired form factor for textile integration.

Indeed, the recent substantial progress in engineering materials with unprecedented thermoelectric efficiencies has not yet evolved into the emergence of thermoelectric devices with sizable performance improvement. Currently, commercial thermoelectric devices are fabricated similarly as they were made fifty years ago. New device architectures that allow integration of high-efficiency thermoelectric materials, can maintain a high-temperature differential in a low-profile geometry and produce large voltage output, such as thin-film quasi-planar designs, are highly desired for wearables and textile integration [210]. Such devices can generate orders of magnitude larger voltage and mitigate the poor performance of the DC-DC boost converters at low voltages.

11. Conclusion

The application of body energy harvesters for powering wearables is a new field, which still requires further research and development to create a viable technology. Wearable devices powered by body energy can reduce the global environmental impact of batteries and save millions of dollars in energy costs per year. Such devices are expected to have broad market acceptance by eliminating the need for frequent charging of the wearable devices. The mode of action and the resulting output power of different active and passive harvesters appropriate for harvesting energy from human body were discussed and compared where applicable. Thermoelectric generators are passive harvesters because they require no action from the wearer and harness the body temperature. They seem to be the closest technology for integration into wearable systems with several products already been introduced to the market. Small and lightweight thermoelectric generators can be integrated into wearable devices making continuous and long-term monitoring a reality. For such devices to become market acceptable, several crucial requirements must be met such as body comfort, form factor, durability, reliability, cost, figure-of-merit, and ease of operation dictated by the end application.

To date, thermoelectric material research has been mostly progressing independently from the application needs. The commercial devices do not have the optimum geometry or form factor desired for wearability. For wearables, further developments require materials that are designed and optimized specifically to meet the device and system-level requirements. Low profile device architectures that can maintain significant temperature differential and simultaneously generate large voltage output can make wearable thermoelectric generators more attractive for textile integration.

Finally, it is worth mentioning that for the integration of wearable harvesters and devices into textiles become a reality, the comfort clothing, and aesthetic factors should not be compromised. For example, the size of the thermoelectric generator or any other energy harvester integrated into textile must be scaled so that the harvester can generate the required electrical power. Several small rigid thermoelectric generator may produce more power than a large area printed thermoelectric generator covering the whole body. A device that can make $10\,\mu W/cm^2$ can be $1000\times$ smaller than one that can make $10\,nW/cm^2$. Therefore, this seems logical that device efficiency becomes a central issue so that the technical wearable designs remain in compliance with the comfortability and market acceptance.

Acknowledgements

This study is partially based upon work supported by the National Science Foundation (NSF) under grant numbers EEC-1160483, ECCS-1351533 and CMMI-1363485.

References

[1] Atzori L, Iera A, Morabito G. The internet of things: a survey. Comput Netw 2010;54:2787–805.
[2] Misra V, Bozkurt A, Calhoun B, Jackson T, Jur JS, Lach J, et al. Flexible technologies for self-powered wearable health and environmental sensing. Proc IEEE 2015;103:665.
[3] Castano LM, Flatau AB. Smart fabric sensors and e-textile technologies: a review. Smart Mater Struct 2014;23:053001.
[4] Hiremath Sh, Yang G, Mankodiya K. Wearable Internet of Things: concept, architectural components and promises for person-centered healthcare. 2014 EAI 4th international conference on wireless mobile communication and healthcare (Mobihealth). IEEE; 2014.
[5] Maleville C. Engineered substrates for Moore and more than Moore's law device scaling: entering the substrate era. 2015 IEEE SOI-3D-subthreshold microelectronics technology unified conference (S3S). 2015.
[6] Ando Junior OH, Maran ALO, Henao NC. A review of the development and applications of thermoelectric microgenerators for energy harvesting. Renew Sustain Energy Rev 2018;91:376–93.
[7] Roundy S, Trolier-McKinstry S. Materials and approaches for on-body energy harvesting. MRS Bull 2018;43:206–13.
[8] Suarez F, Nozariasbmarz A, Vashaee D, Öztürk MC. Designing thermoelectric generators for self-powered wearable electronics. Energy Environ Sci 2016;9:2099–113.
[9] Leonov V, Torfs T, Fiorini P, Van Hoof C. Thermoelectric converters of human warmth for self-powered wireless sensor nodes. IEEE Sens J 2007;7:650–7.
[10] Leonov V. Thermoelectric energy harvesting of human body heat for wearable sensors. IEEE Sens J 2013;13(6).
[11] Bahk J-H, Fang H, Yazawa K, Shakouri A. Flexible thermoelectric materials and device optimization for wearable energy harvesting. J Mater Chem C 2015;3:10362–74.
[12] Leonov V, Vullers RJM. Wearable electronics self-powered by using human body heat: the state of the art and the perspective. J Renew Sustain Energy 2009;1:062701.
[13] Zhou M, Al-Furjana MSH, Zou J, Liu W. A review on heat and mechanical energy harvesting from human – principles, prototypes and perspectives. Renew Sustain Energy Rev 2018;82:3582–609.
[14] Priya S, Inman DJ. Energy harvesting technologies. Boston (MA): Springer; 2009.
[15] Tadesse Y, Zhang S, Priya S. Multimodal energy harvesting system: piezoelectric and electromagnetic. J Intell Mater Syst Struct 2009;20(5):625–32.
[16] Roundy S. On the effectiveness of vibration-based energy harvesting. J Intell Mater Syst Struct 2005;16(10):809–23.
[17] Vullers RJM, van Schaijk R, Doms I, Van Hoof C, Mertens R. Micropower energy harvesting. Solid-State Electron 2009;53:684–93.
[18] Riemer R, Shapiro A. Biomechanical energy harvesting from human motion: theory, state of the art, design guidelines and future directions. J Neuroeng Rehabil 2011;8:1–13.
[19] Winter DA. Biomechanics and motor control of human movement. 3 ed. Hoboken (NJ): John Wiley and Sons; 2005.
[20] Wilson S. Wearable Momentum Continues. CCS Insight; 17 Feb. 2016. www.ccsinsight.com/press/company-news/2516-wearables-momentum-continues [accessed 27 Aug. 2018].
[21] Lamkin P. Wearable tech market to be worth $34 billion by 2020. Forbes; 17 Feb. 2020. www.forbes.com/sites/paullamkin/2016/02/17/wearable-tech-market-to-be-worth-34-billion-by-2020/#3b8bcacc3cb5 [accessed 27 Aug. 2018].
[22] Llamas R, et al. Worldwide wearables market to nearly double by 2021. International Data Corporation (IDC); 2017. https://www.idc.com/getdoc.jsp?containerId=prUS42818517.
[23] Casselman J, et al. Wearable healthcare: lessons from the past and a peek into the future. Telematics Inform 2017;34(7):1011–23.
[24] At the gate and beyond: outlook for the sports market in North America through 2021. United States: Pricewaterhouse Coopers (PwC) LLP; 2017, p. 1–15. https://www.pwc.com/us/en/industry/entertainment-media/publications/assets/pwc-sports-outlook-2017.pdf.
[25] CES® 2018 product offerings: consumer technology association; 2018, p. 1–80. https://ces.tech/.
[26] Rohan M. Thermoelectric generators market worth 547.7 million USB by 2020. CISION PR Newswire, PR Newswife Association LLC; 2015. www.prnewswire.com/news-releases/.thermoelectric-generators-market-worth-5477-million-usd-by-2020-528044901.html [accessed 27 Aug. 2018].
[27] Smart textiles/fabrics market worth $9.3 billion by 2024. Grand View Research Inc.; 2015. https://www.grandviewresearch.com/press-release/global-smart-textiles-industry.
[28] Hyland M, Hunter H, Liu J, Veety E, Vashaee D. Wearable thermoelectric generators for human body heat harvesting. Appl Energy 2016;182:518–24.
[29] Qi Y, McAlpine MC. Nanotechnology-enabled flexible and biocompatible energy harvesting. Energy Environ Sci 2010;3:1275–85.
[30] Shinohara Y. Recent progress of thermoelectric devices or modules in Japan. Mater Today: Proc 2017;4(12):12333.
[31] Ferrari M, Ferrari V, Guizzetti M, Marioli D, Taroni A. Characterization of thermoelectric modules for powering autonomous sensors. Proceedings of IMTC 2007 instrumentation and measurement technology conference. 2007.
[32] Matrix powerwatch. Powerwatch, Matrix Industries. www.powerwatch.com/ [accessed 27 Aug. 2018].
[33] IoT and wearables powered by heat. Matrix Industries. www.matrixindustries.com/ [accessed 27 Aug. 2018].
[34] Yap YZ, et al. Thermoelectric energy harvesting for mobile phone charging application. 2016 IEEE region 10 conference (TENCON), Singapore. 2016. p. 3241–5.
[35] Bunker A. Vodafone unveils the future of festival season tech: charge your phone while you sleep. Vodafone Limited. 2013. blog.vodafone.co.uk/2013/06/12/.vodafone-unveils-the-future-of-festival-season-tech-charge-your-phone-while-you-sleep/ [accessed 27 Aug. 2018].
[36] Van Bavel M, et al. Wearable battery-free wireless 2-channel EEG systems powered by energy scavengers. Sens. Transd. J. 2008;94(7):103.
[37] Thielen M, et al. Thermoelectric energy harvesting for energy autonomous active EEG electrodes. 34th international conference on thermoelectrics (ICT 2015), Dresden, Germany. 2015.
[38] GreenTEG AG offering of core body temperature sensors. Technopark Zurich (Zurich, Switzerland): Presentation to the "Fytbyt" CPO; 2018. https://www.cips.org/Documents/Membership/Branch%20Speaker%20Presentations/3_greenTEG.pdf.
[39] Invernizzi F, et al. Energy harvesting from human motion: materials and techniques. Chem Soc Rev 2016;45(20):5455–73.
[40] Liu Y. Active energy harvesting. Ph.D. Dissertation. The Pennsylvania State University; 2006, https://etda.libraries.psu.edu/catalog/7392.
[41] Liu Y, et al. Active piezoelectric energy harvesting: general principle and experimental demonstration. J Intell Mater Syst Struct 2008;20(5):575–85.
[42] Howells CA. Piezoelectric energy harvesting. Energy Convers Manage 2009;50(7):1847–50.
[43] Toprak A, Tigli O. Piezoelectric energy harvesting: state-of-the-art and challenges. Appl Phys Rev 2014;1(3):031104.
[44] Zhou M, et al. A review on heat and mechanical energy harvesting from human – principles, prototypes and perspectives. Renew Sustain Energy Rev 2018;82:3582–609.
[45] Xue T, Yeo HG, Trolier-McKinstry S, Roundy S. Wearable inertial energy harvester with sputtered bimorph lead zirconate titanate (PZT) thin-film beams. Smart Mater Struct 2018;27:085026. [12pp].
[46] Yeo HG, Xue T, Roundy S, Ma X, Rahn C, Trolier-McKinstry S. Strongly (001) oriented bimorph PZT film on metal foils grown by rf-sputtering for wrist-worn piezoelectric energy harvesters. Adv Funct Mater 2018;28(36):1801327.
[47] Bouendeu E, et al. A low-cost electromagnetic generator for vibration energy

harvesting. IEEE Sens J 2011;11(1):107–13.
[48] Du L, et al. Review of micro magnetic generator. Sens Transd J 2014;176:1–12.
[49] Hannan MA, et al. Energy harvesting for the implantable biomedical devices: issues and challenges. Biomed Eng Online 2014;13(1):79.
[50] Li WJ, et al. Infrared signal transmission by a laser-micromachined, vibration-induced power generator. IEEE Operations Center, Proceedings of the 43rd IEEE midwest symposium on circuits and systems: August 8–11, 2000. Lansing (MI): Lansing Convention Center; 2000.
[51] Kymissis J, et al. Parasitic power harvesting in shoes. IEEE Computer Society Press, Second international symposium on wearable computers: digest of papers, October 1998, Pittsburgh, Pennsylvania. 1998.
[52] Hayashida JY. Unobtrusive integration of magnetic generator systems into common footwear. Department of Mechanical Engineering, Massachusetts Institute of Technology; 2000.
[53] Buren TV, et al. Optimization of inertial micropower generators for human walking motion. IEEE Sens J 2006;6(1):28–38.
[54] Kim BJ, Kim DH, Lee Y-Y, Shin H-W, Han GS, Hong JS, et al. Highly efficient and bending durable perovskite solar cells: toward a wearable power source. Energy Environ Sci 2015;8:916–21.
[55] Yi F, Zhang Z, Kang Z, Liao Q, Zhang Y. Recent advances in triboelectric nanogenerator-based health monitoring. Adv Funct Mater 2019:1808849.
[56] Hu X, Huang Z, Zhou X, Li P, Wang Y, Huang Z, et al. Wearable large-scale perovskite solar-power source via nanocellular scaffold. Adv Mater 2017;29:1703236.
[57] Dieffenderfer JP, Beppler E, Novak T, Whitmire E, Jayakumar R, Randall C, et al. Solar powered wrist worn acquisition system for continuous photoplethysmogram monitoring. Proc 36th Int Conf IEEE Eng Med Biol Soc (EMBC'14), Chicago, IL. 2014.
[58] Pan S, Yang Z, Chen P, Deng J, Li H, Peng H. Wearable solar cells by stacking textile electrodes. Angew Chem Int Ed 2014;53:6110–4.
[59] Fan F-R, Tian Z-Q, Wang ZL. Flexible triboelectric generator!. Nano Energy 2012;1:328–34.
[60] Wu F, Li C, Yin Y, Cao R, Li H, Zhang X, et al. Lightweight, and wearable triboelectric nanogenerator for energy harvesting and self-powered sensing. Adv Mater Technol 2019;4:1800216.
[61] Hinchet R, Seung W, Kim S-W. Energy harvesting from human motion: materials and techniques. ChemSusChem 2015;8:2327.
[62] Zhu G, Zhou YS, Bai P, Meng XS, Jing Q, Chen J, et al. A shape-adaptive thin-film-based approach for 50% high-efficiency energy generation through micro-grating sliding electrification. Adv Mater 2014;26:3788–96.
[63] Invernizzi F, Dulio S, Patrini M, Guizzetti G, Mustarelli P. Energy harvesting from human motion: materials and techniques. Chem Soc Rev 2016;45:5455.
[64] Potnuru A, Tadesse Y. Characterization of pyroelectric materials for energy harvesting from human body. Integr Ferroelectr 2014;150(1):23–50.
[65] Bell LE. Cooling, heating, generating power, and recovering waste heat with thermoelectric systems. Science Dec. 2008;321(5895):1457–61.
[66] Lou Z, et al. Wearable sensors: recent progress of self-powered sensing systems for wearable electronics (Small 45/2017). Small 2017;13(45).
[67] Navid A, Pilon L. Pyroelectric energy harvesting using olsen cycles in purified and porous poly(vinylidene fluoride-trifluoroethylene) [P(VDF-TrFE)] thin films. Smart Mater Struct 2011;20(2):025012.
[68] Bowen CR, et al. Pyroelectric materials and devices for energy harvesting applications. Energy Environ Sci 2014;7(12):3836–56.
[69] Yang Y, et al. Pyroelectric nanogenerators for driving wireless sensors. Nano Lett 2012;12(12):6408–13.
[70] Kim M-S, et al. Modeling of a honeycomb-shaped pyroelectric energy harvester for human body heat harvesting. Smart Mater Struct 2015;24(6):065032.
[71] Twaha S, Zhu J, Yan Y, Li B. A comprehensive review of thermoelectric technology: materials, applications, modelling and performance improvement. Renew Sustain Energy Rev 2016;65:698–726.
[72] Kütt L, Millar J, Karttunen A, Lehtonen M, Karppinen M. Thermoelectric applications for energy harvesting in domestic applications and micro-production units. Part I: thermoelectric concepts, domestic boilers and biomass stoves. Renew Sustain Energy Rev 2017. [in press].
[73] Oh JY, et al. Chemically exfoliated transition metal dichalcogenide nanosheet-based wearable thermoelectric generators. Energy Environ Sci 2016;9(5):1696–705.
[74] Wan C, et al. Flexible thermoelectric foil for wearable energy harvesting. Nano Energy 2016;30:840–5.
[75] Shi Y, et al. Design and fabrication of wearable thermoelectric generator device for heat harvesting. IEEE Rob Autom Lett 2018;3(1):373–8.
[76] Leonov V. Thermoelectric energy harvesting of human body heat for wearable sensors. IEEE Sens J 2013;13(6):2284–91.
[77] Settaluri KT, et al. Thin thermoelectric generator system for body energy harvesting. J Electron Mater Oct. 2011;41(6):984–8.
[78] Vashaee D, Nozariasbmarz A, et al. Thermoelectric generators for body heat harvesting. In: The 35th international conference and the 1st asian conference on thermoelectrics (ICT/ACT 2016); 2016. www.its.org/content/35th-international-conference-and-1st-asian-conference-thermoelectrics-ictact-2016-first.
[79] Jo SE, et al. Flexible thermoelectric generator for human body heat energy harvesting. Electron Lett 2012;48(16):1015–7.
[80] Wang Z, et al. Realization of a wearable miniaturized thermoelectric generator for human body applications. Sens Actuat A 2009;156(1):95–102.
[81] Jo S-E, et al. Human body heat energy harvesting using flexible thermoelectric generator for autonomous microsystems. 16th international conference on miniaturized systems for chemistry and life sciences (MicroTAS 2012): Okinawa, Japan, 28 October–1 November 2012. 2014.
[82] Kim M-K, et al. Wearable thermoelectric generator for harvesting human body heat energy. Smart Mater Struct 2014;23(10):105002.
[83] Im HK, et al. Flexible thermocells for utilization of body heat. Nano Res 2014;7(4):443–52.
[84] Strasser M, et al. Micromachined CMOS thermoelectric generators as on-chip power supply. Sens Actuat A 2004;114(2–3):362–70.
[85] Wahbah M, et al. Characterization of human body-based thermal and vibration energy harvesting for wearable devices. IEEE J Emerg Sel Top Circ Syst 2014;4(3):354–63.
[86] Siddique ARM, et al. Thermal energy harvesting from the human body using flexible thermoelectric generator (FTEG) fabricated by a dispenser printing technique. Energy 2016;115:1081–91.
[87] Nozariasbmarz A, Kishore RA, Poudel B, Saparamadu U, Li W, Cruz R, et al. ACS Appl Mater Interfaces 2019. https://doi.org/10.1021/acsami.9b14823.
[88] Magno M, Boyle D. Wearable energy harvesting: from body to battery. 12th international conference on design & technology of integrated systems in nanoscale era (DTIS), Palma de Mallorca. 2017. p. 1–6.
[89] Sarker MR, et al. Modelling and simulation an AC-DC rectifier circuit based on piezoelectric vibration sensor for energy harvesting system. Appl Mech Mater 2015;785:131–5.
[90] Ramadass YK, Chandrakasan AP. An efficient piezoelectric energy harvesting interface circuit using a bias-flip rectifier and shared inductor. IEEE J Solid-State Circ 2010;45(1):189–204.
[91] Liu L, et al. A self-powered piezoelectric energy harvesting interface circuit with efficiency-enhanced P-SSHI rectifier. J Semicond 2018;39(4):045002.
[92] Badel A, et al. Piezoelectric energy harvesting using a synchronized switch technique. J Intell Mater Syst Struct 2006;17(8–9):831–9.
[93] Richelli A, et al. A 0.2-1.2V DC/DC boost converter for power harvesting applications. IEEE Trans Power Electron 2009;24(6):1541–6.
[94] Chowdary G, Chatterjee S. A 300-nW sensitive, 50-nA DC-DC converter for energy harvesting applications. IEEE Trans Circuits Syst I Regul Pap Nov. 2015;62(11):2674–84.
[95] Ahmed KZ, Mukhopadhyay S. Awide conversion ratio, extended input 3.5-μA boost regulator with 82% efficiency for low-voltage energy harvesting. IEEE Trans Power Electron 2014;29(9):4776–86.
[96] Ostfeld AE, Gaikwad AM, Khan Y, Arias AC. High-performance flexible energy storage and harvesting system for wearable electronics. Sci Rep 2016;6:26122.
[97] Dong L, Xu C, Li Y, Huang Z-H, Kang F, Yang Q-H, et al. Flexible electrodes and supercapacitors for wearable energy storage: a review by category. J Mater Chem A 2016;4:4659–85.
[98] Lee Y-H, Kim J-S, Noh J, Lee I, Kim HJ, Choi S, et al. Wearable textile battery rechargeable by solar energy. Nano Lett 2013;13:5753–61.
[99] Im JP, et al. A 40 mV transformer-reuse self-startup boost converter with MPPT control for thermoelectric energy harvesting. IEEE J Solid-State Circ 2012;47(12):3055–67.
[100] Carlson EJ, et al. A 20 mV input boost converter with efficient digital control for thermoelectric energy harvesting. IEEE J Solid-State Circ 2010;45(4):741–50.
[101] Bandyopadhyay S, Chandrakasan AP. Platform architecture for solar, thermal, and vibration energy combining with MPPT and Single inductor. IEEE J Solid-State Circ 2012;47(9):2199–215.
[102] Shrivastava A, et al. A 10 mV-input boost converter with inductor peak current control and zero detection for thermoelectric and solar energy harvesting with 220 mV cold-start and 14.5 dBm, 915 MHz RF kick-start. IEEE J Solid-State Circ 2015;50(8):1820–32.
[103] Goeppert J, Manoli Y. Fully integrated startup at 70 mV of boost converters for thermoelectric energy harvesting. IEEE J Solid-State Circ 2016;51(7):1716–26.
[104] Meli M, Dillersberger H. Efficiently harvesting energy from temperature differences in order to power wireless systems. Proceedings of the wireless congress, Munich. 2014. p. 1–8.
[105] Guyton A, Hall J. Textbook of medical physiology, 11th; 2006.
[106] Gagge AP, Gonzalez RR. Mechanisms of heat exchange: biophysics and physiology. Handbook of physiology, section 4; 1996, p. 45–84.
[107] Kelly G. Body temperature variability (Part 1): a review of the history of body temperature and its variability due to site selection, biological rhythms, fitness, and aging. Altern Med Rev 2006;11(4):278.
[108] Gagge AP, et al. Comfort and thermal sensations and associated physiological responses at various ambient temperatures. Environ Res 1967;1(1):1–20.
[109] Saggin B, Tarabini M, Lanfranchi G. A device for the skin-contact thermal resistance measurement. IEEE Trans Instrum Meas 2012;61(2):489–95.
[110] Smith CE. A transient, three-dimensional model of the human thermal system. ProQuest Dissertations Publishing; 1991.
[111] Gagge AP, Nishi Y. Heat exchange between human skin surface and thermal environment. Comprehensive physiology; 2011.
[112] Leonov V, Vullers RJM. Thermoelectric generators on living beings. Proceedings of the 5th European conference on thermoelectrics (ECT), Odessa, Ukraine. 2007.
[113] Fiala D, et al. A computer model of human thermoregulation for a wide range of environmental conditions: the passive system. J Appl Physiol 1999;87(5):1957–72.
[114] Lee D, Park H, Park G, Kim J, Kim H, Cho H, Kim W. Liquid-metal-electrode-based compact, flexible, and high-power thermoelectric device. Energy 2019;188:116019.
[115] Park H, Eom Y, Lee D, Kim J, Kim H, Park G, Kim W. High power output based on watch-strap-shaped body heat harvester using bulk thermoelectric materials. Energy 2019;187:115935.
[116] Pennes HH. Analysis of tissue and arterial blood temperatures in the resting human forearm. J Appl Physiol 1948;1(2):93–122.

[117] Chen MM, Holmes KR. Microvascular contributions in tissue heat transfer. Ann N Y Acad Sci 1980;335:137–50.
[118] Weinbaum S, Jiji LM. A new simplified bioheat equation for the effect of blood flow on local average tissue temperature. J Biomech Eng 1985;107(2):131–9.
[119] Wijethunge D, et al. Simplified human thermoregulatory model for designing wearable thermoelectric devices. J Phys D Appl Phys 2017;51:055401.
[120] Salloum M, et al. A new transient bioheat model of the human body and its integration to clothing models. Int J Therm Sci 2007;46(4):371–84.
[121] Fiala D, et al. Computer prediction of human thermoregulatory and temperature responses to a wide range of environmental conditions. Int J Biometeorol 2001;45(3):143–59.
[122] DiSalvo FJ. Thermoelectric cooling and power generation. Science 1999;285:703–6.
[123] Majumdar A. Thermoelectricity in semiconductor nanostructures. Science 2004;303(5659):777–8.
[124] Vining CB. Thermoelectric properties of silicides. CRC handbook of Thermoelectrics; 1995, p. 277–86.
[125] Rowe DM. Thermoelectrics handbook: macro to nano. CRC Press; 2005.
[126] Ioffe AF. Semiconductor thermoelements, and thermoelectric cooling. Infosearch; 1957.
[127] Snyder GJ, Toberer ES. Complex thermoelectric materials. Nat Mater 2008;7(2):105–14.
[128] Minnich AJL, et al. Bulk nanostructured thermoelectric materials: current research and future prospects. Energy Environ Sci 2009;2:466–79.
[129] Dresselhaus MS, et al. New directions for low-dimensional thermoelectric materials. Adv Mater 2007;19:1043–53.
[130] Vineis CJ, et al. Nanostructured thermoelectrics: big efficiency gains from small features. Adv Mater 2010;22(36):3970–80.
[131] He J, Tritt TM. Advances in thermoelectric materials research: looking back and moving forward. Science 2017;357:1369.
[132] Goldsmid HJ. Applications of thermoelectricity. London: Methuen & Co. Ltd; 1960.
[133] Schmidt GR, Wiley RL, Richardson RL. NASA's program for radioisotope power system research and development. Space technology and applications international forum (STAIF 2005), AIP Conference Proceedings 746, Albuquerque, NM, February 14–17. 2005.
[134] Nozariasbmarz A. In-situ sintering decrystallization of thermoelectric materials using microwave radiation PhD. dissertation Raleigh (North Carolina, USA): North Carolina State University; 2017.
[135] Poudel B, et al. High-thermoelectric performance of nanostructured bismuth antimony telluride bulk alloys. Science 2008;320:634–8.
[136] Xu Z, et al. Attaining high mid-temperature performance in (Bi, Sb)2Te3 thermoelectric materials via synergistic optimization. NPG Asia Mater 2016;8. ID. e302.
[137] Kim SI, et al. Dense dislocation arrays embedded in grain boundaries for high-performance bulk thermoelectrics. Science 2015;348:109–14.
[138] Zheng Y, et al. Mechanically robust BiSbTe alloys with superior thermoelectric performance: a case study of stable hierarchical nanostructured thermoelectric materials. Adv Energy Mater 2015;5:1401391.
[139] Xie W, et al. Unique nanostructures and enhanced thermoelectric performance of melt-spun BiSbTe alloys. Appl Phys Lett 2009;94:102111.
[140] Zheng G, et al. High thermoelectric performance of p-BiSbTe compounds prepared by ultra-fast thermally induced reaction. Energy Environ Sci 2017;10:2638.
[141] Pan Y, et al. Mechanically enhanced p- and n-type Bi2Te3-based thermoelectric materials reprocessed from commercial ingots by ball milling and spark plasma sintering. Mat Sci Eng B 2015;197:75–81.
[142] Wang S, et al. Enhanced thermoelectric properties of Bi2(Te1_xSex)3-based compounds as n-type legs for low-temperature power generation. J Mater Chem 2012;22:20943–51.
[143] Yan X, et al. Experimental studies on anisotropic thermoelectric properties and structures of n-type Bi2Te2.7Se0.3. Nano Lett 2010;10:3373.
[144] Liu WS, et al. Thermoelectric property studies on Cu-doped n-type CuxBi2Te2.7Se0.3 nanocomposites. Adv Energy Mater 2011;1(4):1–11.
[145] Song S, et al. Thermoelectric properties of n-type Bi2Te2.7Se0.3 with addition of nano-ZnO: Al particles. Mater Res Exp 2014;1:035901.
[146] Hong M, et al. n–Type Bi2Te3-xSex nanoplates with enhanced thermoelectric efficiency driven by wide frequency phonon scatterings and synergistic carrier scatterings. ACS Nano 2016;10:4719–27.
[147] Hu L, et al. Point defect engineering of high-performance bismuth-telluride-based thermoelectric materials. Adv Funct Mater 2014;24:5211–8.
[148] Liu W, et al. Studies on the Bi2Te3–Bi2Se3–Bi2S3 system for mid-temperature thermoelectric energy conversion. Energy Environ Sci 2013;6:552–60.
[149] Nozariasbmarz A, et al. Engineering of n-type BiSeTe nanostructures by microwave processing for body heat harvesting application; 2019 [in preparation].
[150] Nozariasbmarz A, Krasinski JS, Vashaee D. N-type bismuth telluride nanocomposite materials optimization for thermoelectric generators in wearable applications. Materials 2019;12(9):1529.
[151] Suarez F, et al. Flexible thermoelectric generator using bulk legs and liquid metal interconnects for wearable electronics. Appl Energy 2017;202:736–45.
[152] Eom Y, et al. Flexible thermoelectric power generation system based on rigid inorganic bulk materials. Appl Energy 2017;206:649–56.
[153] Qing S, et al. Characteristics and parametric analysis of a novel flexible ink-based thermoelectric generator for human body sensor. Energy Convers Manage 2018;156:655–65.
[154] Leonov V. Thermoelectric energy harvester on the heated human machine. J Micromech Microeng 2011;21(12):125013.
[155] Leonov V, Vullers RJM. Wearable thermoelectric generators for body-powered devices. J Electron Mater 2009;38(7):1491–8.
[156] Aerogels for thermal insulation of thermoelectric devices. NASA Tech Briefs 2006; 30(7): 50–2.
[157] Bahk J-H, et al. Flexible thermoelectric materials and device optimization for wearable energy harvesting. J Mater Chem C 2015;3(40):10362–74.
[158] Dunham MT, et al. Power density optimization for micro thermoelectric generators. Energy 2015;93:2006–17.
[159] Schmidt M, Schwertfeger F. Applications for silica aerogel products. J Non-Cryst Solids 1998;225:364–8.
[160] Sakamoto J, et al. System and method for fabrication of high-efficiency durable thermoelectric devices. Patent Application No. US 2006/0157101 A1. July 20; 2006.
[161] Aswal DK, et al. Key issues in development of thermoelectric power generators: high figure-of-merit materials and their highly conducting interfaces with metallic interconnects. Energy Convers Manage 2016;114:50–67.
[162] Glatz W, et al. Optimization and fabrication of thick flexible polymer based micro thermoelectric generator. Sens Actuat. A 2006;132(1):337–45.
[163] Glatz W, et al. Bi2Te3-based flexible micro thermoelectric generator with optimized design. J Microelectromech Syst 2009;18(3):763–72.
[164] Liang Gaowei, et al. Analytical model of parallel thermoelectric generator. Appl Energy 2011;88(12):5193–9.
[165] Francioso L, et al. Flexible thermoelectric generator for wearable biometric sensors. 2010 IEEE Sensors. 2010.
[166] Sahin AZ, Yilbas Bekir S. "The thermoelement as thermoelectric power generator: effect of leg geometry on the efficiency and power generation". Energy Convers Manage 2013;65:26–32.
[167] Yazawa K, Shakouri A. Cost-efficiency trade-off and the design of thermoelectric power generators. Environ Sci Technol 2011;45(17):7548–53.
[168] Shannon KY, et al. $ per W metrics for thermoelectric power generation: beyond ZT. Energy Environ Sci 2013;6:2561–71.
[169] Bergmann Tiest WM. An experimentally verified model of the perceived "coldness" of objects. Proc 2nd Joint EuroHaptics Conf Symp World Haptics. 2007. p. 61–5.
[170] Mitcheson PD. Energy harvesting for human wearable and implantable bio-sensors. Proceedings of the IEEE annual international conference on engineering in medicine and biology society (EMBC), September. 2010. p. 3432–6.
[171] Tanabe S, Arens EA, Bauman FS, Zhang H, Madsen TL. Evaluating thermal environments by using a thermal manikin with controlled skin surface temperature. ASHRAE Trans 1994;100(1):39–48.
[172] Leonov V, Fiorini P. Thermal matching of a thermoelectric energy scavenger with the ambient. Proc 5th European conf on thermoelectrics (ECT), Odessa, Ukraine, Sep. 10–12. 2007.
[173] Sharp J, Bierschenk J, Lyon HB. Overview of solid-state thermoelectric refrigerators and possible applications to on-chip thermal management. Proc IEEE 2006;94(8):1602–12.
[174] Lossec M, et al. Thermoelectric generator placed on the human body: system modeling and energy conversion improvements. Eur Phys J Appl Phys 2010;52(1):11103.
[175] Kim SJ, et al. A wearable thermoelectric generator fabricated on a glass fabric. Energy Environ Sci 2014;7(6):1959.
[176] Siddique ARM, et al. A review of the state of the science on wearable thermoelectric power generators (TEGs) and their existing challenges. Renew Sustain Energy Rev 2017;73:730–44.
[177] Navone C, et al. Development of (Bi, Sb)2(Te, Se)3-based thermoelectric modules by a screen-printing process. J Electron Mater Feb. 2010;39(9):1755–9.
[178] Itoigawa K, et al. Fabrication of flexible thermopile generator. J Micromech Microeng 2005;15(9).
[179] Hewitt CA, et al. Multilayered carbon nanotube/polymer composite based thermoelectric fabrics. Nano Lett 2012;12(3):1307–10.
[180] Yang Y, et al. Nanowire-composite based flexible thermoelectric nanogenerators and self-powered temperature sensors. Nano Res 2012;5(12):888–95.
[181] Mortazavinatanzi S, et al. Printing and folding: a solution for high-throughput processing of organic thin-film thermoelectric devices. Sensors 2018;18(4):989.
[182] Weber J, et al. Coin-size coiled-up polymer foil thermoelectric power generator for wearable electronics. Sens Actuat A 2006;132(1):325–30.
[183] Lu Z, et al. Silk fabric-based wearable thermoelectric generator for energy harvesting from the human body. Appl Energy 2016;164:57–63.
[184] Jeong SH, et al. Stretchable thermoelectric generators metallized with liquid alloy. ACS Appl Mater Interfaces 2017;9(18):15791–7.
[185] Kim CS, et al. Structural design of a flexible thermoelectric power generator for wearable applications. Appl Energy 2018;214:131–8.
[186] Park H, et al. High power output from body heat harvesting based on flexible thermoelectric system with low thermal contact resistance. J Phys D Appl Phys 2018;51(36):365501.
[187] Toshima N. Recent progress of organic and hybrid thermoelectric materials. Synth Met 2017;225:3–21.
[188] Chen G, et al. Recent advances in organic polymer thermoelectric composites. J Mater Chem C 2017;5(18):4350–60.
[189] Cowen LM, et al. Review—organic materials for thermoelectric energy generation. ECS J Solid State Sci Technol 2017;6(3):N3080–8.
[190] Yang P, et al. Wearable thermocells based on gel electrolytes for the utilization of body heat. Angew Chem Int Ed 2016;55(39):12050–3.
[191] Du Y, Cai K, Chen S, Wang H, Shen SZ, Danelson R, et al. Thermoelectric fabrics: toward power generating clothing. Sci Rep 2015;5(1):6411.
[192] Lee JA, Aliev AE, Bykova JS, de Andrade MJ, Kim D, Sim HJ, et al. Woven-yarn

thermoelectric textiles. Adv Mater 2016;28(25):5038–44.
[193] Huu TN, et al. Flexible thermoelectric power generator with Y-type structure using electrochemical deposition process. Appl Energy 2018;210:467–76.
[194] Kim SJ, Lee HE, Choi H, Kim Y, We JH, Shin JS, et al. High-performance flexible thermoelectric power generator using laser multiscanning lift-off process. ACS Nano 2016;10(12):10851–7.
[195] Liu J, et al. Flexible thermoelectric generators compatible with commercial module fabrication processes international conference on thermoelectrics. ICT2017, California, USA, Jul. 30th to Aug. 3rd; 2017.
[196] Pu X, Hu W, Wang ZL. Toward wearable self-charging power systems: the integration of energy-harvesting and storage devices. Small 2018;14:1702817.
[197] AiQ Smart Clothing. Bouncin. www.aiqsmartclothing.com/product-service/ [accessed 27 Aug. 2018].
[198] MYANT. myant.ca/technology/ [accessed 27 Aug. 2018].
[199] Ohmatex Smart Textile R&D Consultants. Ohmatex, Himmelblaa, www.ohmatex.dk/ [accessed 27 Aug. 2018].
[200] Zhang L, Lin S, Hua T, Huang B, Liu S, Tao X. Fiber-based thermoelectric generators: materials, device structures, fabrication, characterization, and applications. Adv Energy Mater 2018;8:1700524.
[201] Mills AC, Hodges R, Jur JS. Human and environment influences on thermoelectric energy harvesting toward self-powered textile-integrated wearable devices. MRS Adv 2016;1(38):2665–70.
[202] Kim J-Y, Lee W, Hun Y, Song K, Cho Y, Jang K-S. Wet-spinning and post-treatment of CNT/PEDOT:PSS composites for use in organic fiber-based thermoelectric generators. Carbon 2018;133:293.
[203] Kim M-K, Kim M-S, Lee S, Kim C, Kim Y-J. Wearable thermoelectric generator for harvesting human body heat energy. Smart Mater Struct 2014;23:105002.
[204] Wang Y, Shi Y, Mei D, Chen Z. Wearable thermoelectric generator to harvest body heat for powering a miniaturized accelerometer. Appl Energy 2018;215:690–8.
[205] Kim YJ, Kim SJ, Choi H, Kim CS, Lee G, Park SH, et al. Realization of high-performance screen-printed flexible thermoelectric generator by improving contact characteristics. Adv Mater Interfaces 2017;4:1700870.
[206] Shin S, Kumar R, Roh JW, Ko D-S, Kim H-S, Kim SI, et al. High-performance screen-printed thermoelectric films on fabrics. Sci Rep 2017;7:1–7.
[207] Wu Q, Hu J. Waterborne polyurethane based thermoelectric composites and their application potential in wearable thermoelectric textiles. Compos B Eng 2016;107:59–66.
[208] Embrlabs. Embr Wave: https://embrlabs.com/ [accessed on September 15, 2018].
[209] dhama innovations: http://www.dhamainnovations.com/store [accessed on September 15, 2018].
[210] Vashaee D, Liu J, Ozturk M. Thin Film Thermoelectric Generator - Thermoelectric device employing vacuum self-sealing and in-plane thin film structure, and method of fabrication, Photo-enhanced thin-film thermoelectric energy generator, and method of fabrication. Provisional Patent, Docket No. 221404-8380; 2016.